

# The Three Node Wireless Network: Achievable Rates and Cooperation Strategies

Lifeng Lai, Ke Liu, and Hesham El Gamal

{lail,liuk,helgamal}@ece.osu.edu

## Abstract

We consider a wireless network composed of three nodes and limited by the half-duplex and total power constraints. This formulation encompasses many of the special cases studied in the literature and allows for capturing the common features shared by them. Here, we focus on three special cases, namely 1) Relay Channel, 2) Multicast Channel, and 3) Conference Channel. These special cases are judiciously chosen to reflect varying degrees of complexity while highlighting the common ground shared by the different variants of the three node wireless network. For the relay channel, we propose a new cooperation scheme that exploits the wireless feedback gain. This scheme combines the benefits of decode-and-forward and compress-and-forward strategies and avoids the idealistic feedback assumption adopted in earlier works. Our analysis of the achievable rate of this scheme reveals the diminishing feedback gain at both the low and high signal-to-noise ratio regimes. Inspired by the proposed feedback strategy, we identify a greedy cooperation framework applicable to both the multicast and conference channels. Our performance analysis reveals several *nice* properties of the proposed greedy approach and the central role of cooperative source-channel coding in exploiting the receiver side information in the wireless network setting. Our proofs for the cooperative multicast with side-information rely on novel nested and independent binning encoders along with a list decoder.

## I. INTRODUCTION

We are in the midst of a new wireless revolution, brought on by the adoption of wireless networks for consumer, military, scientific, and wireless applications. For example, the consumer potential is clearly evident in the exploding popularity of wireless LANs and Bluetooth-protocol

The authors are with the ECE Department at the Ohio State University. This work was funded in part by the National Science Foundation under Grants CCR 0118859, ITR 0219892, and CAREER 0346887.

devices. The military potential is also clear: wireless networks can be rapidly deployed, and the failure of individual nodes does not imply the failure of the network. Scientific data-collection applications using wireless sensor networks are also gaining in numbers. These applications have sparked a renewed interest in network information theory. Despite the recent progress ( see [1], [2], [3], [4], [10] and references therein), developing a unified theory for network information flow remains an elusive task.

In our work, we consider, perhaps, the most simplified scenario of wireless networks. Our network is composed of only three nodes and limited by the half-duplex and total power constrains. Despite this simplicity, this model encompasses many of the special cases that have been extensively studied in the literature. These special *channels*<sup>1</sup> are induced by the traffic generated at the nodes and the requirements imposed on the network<sup>2</sup>. More importantly, this model exposes the common features shared by these special cases and allows for constructing universal cooperation strategies that yield significant performance gains. In particular, we focus here on three special cases, namely 1) Relay Channel, 2) Multicast Channel, and 3) Conference Channel. These channels are defined rigorously in Section II. We adopt a greedy framework for designing cooperation strategies and characterize the achievable rates of the proposed schemes. Our analysis reveals the structural similarities of the proposed strategies, in the three special cases, and establishes the asymptotic optimality of such strategies in several cases. More specifically, our contributions can be summarized as follows.

- 1) We propose a novel cooperation strategy for the relay channel with feedback. Our scheme combines the benefits of both the decode-and-forward (DF) and compress-and-forward (CF) strategies and avoids the idealistic assumptions adopted in earlier works. Our analysis of the achievable rate of the proposed strategy reveals the diminishing gain of feedback in the asymptotic scenarios of low and large signal-to-noise ratio. We further establish the sub-optimality of orthogonal cooperation strategies ( [7], [18]) in this **half duplex** setting.
- 2) Inspired by the feedback strategy for the relay channel, we construct a greedy cooperation strategy for the multicast scenario. Motivated by a greedy approach, we show that the *weak*

<sup>1</sup>With a slight abuse of notation, we interchange “channel” and “network” in different places of the sequel for maximal consistency with the literature.

<sup>2</sup>For example, the relay channel corresponds to the special case where the traffic is generated at one node and is required to be transmitted to only one of the remaining two nodes.

receiver is led to help the *strong* receiver first<sup>3</sup>. Based on the same greedy motivation, the strong user starts to assist the weak receiver after successfully decoding the transmitted codeword. We compute the corresponding achievable rate achieved by and use it to establish the significant gains offered by this strategy, as compared with the non-cooperative scenario.

- 3) Motivated by the sensor networks application, we identify the conference channel model as a special case of our general formulation. In this model, the three nodes observe correlated data streams and every node wishes to communicate its observations to the other two nodes. Our proposed cooperation strategy in this scenario consists of three stages of *multicast with side information*, where the multicasting order is determined by a low complexity greedy scheduler. In every stage, we use a cooperation strategy obtained as a generalization of the greedy multicast approach. This strategy highlights the central role of cooperative source-channel coding in exploiting the side information available at the receivers. By contrasting the minimum energy required by the proposed strategy with the genie-aided and non-cooperative schemes, we establish its superior performance.
- 4) We identify the greedy principle as the basis for constructing efficient cooperation strategies in the three considered scenarios. Careful consideration of other variants of the three node network reveals the fact that such principle carries over with slight modifications.

The rest of the paper is organized as follows. Section II introduces our modelling assumptions and notation. In Section III, we present the new cooperation strategy for the wireless relay channel with *realistic* feedback and analyze its performance. Building on the relay channel strategy, Section IV develops the greedy cooperation framework for the multi-cast channel. We devote Section V to the conference channel. Finally, we offer some concluding remarks on Section VI. To enhance the flow of the paper, all the proofs are collected in the Appendices.

## II. THE THREE NODE WIRELESS NETWORK

Figure 1 illustrates a network consisting of three nodes each observing a different source. In the general case, the three sources can be correlated. Nodes are interested in obtaining a subset or all the source variables at the other nodes. To achieve this goal, nodes are allowed to

<sup>3</sup>The notions of weak and strong receivers will be defined rigorously in the sequel.

coordinate and exchange information over the wireless channel. Mathematically, the three node wireless network studied in this paper consists of following elements:

- 1) The three sources  $S_i, i = 1, 2, 3$ , drawn i.i.d. from certain known joint distribution  $p(s_1, s_2, s_3)$  over a **finite** set  $\mathcal{S}_1 \times \mathcal{S}_2 \times \mathcal{S}_3$ . We denote by  $S_i^K$  the length- $K$  discrete source sequence  $S_i(1), \dots, S_i(K)$  at the  $i$ -th node. Throughout the sequel, we use capital letters to refer to random variables and small letters for realizations.
- 2) We consider the discrete-time *additive white Gaussian noise* (AWGN) channel. At time instant  $n$ , node  $j$  receives

$$Y_j(n) = \sum_{i \neq j} h_{ji} X_i(n) + Z_j(n) \quad (1)$$

where  $X_i(n)$  is the transmitted signal by node- $i$  and  $h_{ji}$  is the channel coefficient from node  $i$  to  $j$ . To simplify the discussion, we assume the channel coefficients are symmetric, i.e.,  $h_{ij} = h_{ji}$ . These channel gains are assumed to be known *a-priori* at the three nodes. We also assume that the additive zero-mean Gaussian noise is spatially and temporally white and has the same unit variance ( $\sigma^2 = 1$ ).

- 3) We consider half-duplex nodes that cannot transmit and receive *simultaneously* using the same degree of freedom. Without loss of generality, we split the degrees of freedom available to each node in the temporal domain, so that, at each time instant  $n$ , a node- $i$  can either transmit (*T-mode*,  $Y_i(n) = 0$ ) or receive (*R-mode*,  $X_i(n) = 0$ ), but never both. Due to the half-duplex constraint, at any time instant, the network nodes are divided into two groups: the T-mode nodes (denoted by  $\mathcal{T}$ ) and the R-mode nodes ( $\mathcal{R}$ ). A partition  $(\mathcal{T}, \mathcal{R})$  is called a network state.
- 4) Let  $P_i^{(l)}$  denote the average transmit power at the  $i$ -th node during the  $m_l$  network state. We adopt a short-term power constraint such that the total power of all the T-mode nodes at any network state is limited to  $P$ , that is,

$$\sum_{i \in \mathcal{T}_l} P_i^{(l)} \leq P, \quad \forall m_l. \quad (2)$$

- 5) We associate with node- $i$  an index set  $I_i$ , such that  $j \in I_i$  indicates that node- $i$  is interested in obtaining  $S_j$  from node- $j$  ( $j \neq i$ ).
- 6) At node- $i$ , a causal joint source-channel encoder converts a length- $K$  block of source sequence into a length- $N$  codeword. The encoder output at time  $n$  is allowed to depend

on the received signal in the previous  $n - 1$  instants, i.e.,

$$X_i(n) = f_i(n, S_i^K, Y_i^{n-1}). \quad (3)$$

In the special case of a separate source-channel coding approach, the encoder decomposes into:

- A source encoder  $f_{si}$  maps  $S_i^K$  into a node message  $W_i$ , i.e.,  $W_i = f_{si}(S_i^K)$ ,  $W_i \in [1, M_i]$ .
- A channel encoder  $f_{ci}(n)$  encodes the node message into a channel input sequence  $X_i(n) = f_{ci}(n, W_i, Y_i^{n-1})$ .

7) At node- $i$ , decoder  $d_i$  estimates the source variables indexed by  $I_i$

$$\{\hat{S}_{ij}^K\} = d_i(Y_i^N, S_i^K), \quad \forall j \in I_i \quad (4)$$

where  $\hat{S}_{ij}^K$  denotes the estimation of  $S_j^K$  at node  $i$ . In the case of a separate source-channel coding scheme, decoder  $d_i$  consists of the following:

- A channel decoder  $d_{ci}$ ,  $\hat{W}_{ij} = d_{ci}(Y_i^N)$ .
- A source decoder  $d_{si}$ ,  $\hat{S}_{ij}^K = d_{si}(\hat{W}_{ij}, S_i^K)$ .

8) A decoding error is declared if any node fails to reconstruct its intended source variables correctly. Thus, the **joint** error probability can be expressed as

$$P_e^{N,K} = \text{Prob}\left\{ \bigcup_{j \in I_i, i=1,2,3} \{\hat{S}_{ij}^K \neq S_j^K\} \right\}. \quad (5)$$

In the case of a separate coding scheme, the error probability reduces to

$$P_e^N = \text{Prob}\left\{ \bigcup_{j \in I_i, i=1,2,3} \{\hat{W}_{ij} \neq W_j\} \right\}. \quad (6)$$

9) An efficient cooperation strategy should strive to maximize the achievable rate given by  $\frac{KH(S_1, S_2, S_3)}{N}$ , where  $N$  is the minimum number of channel uses necessary to satisfy the network requirements. For a fixed  $H(S_1, S_2, S_3)$ , this optimization is equivalent to minimizing the bandwidth expansion factor  $\tau = \frac{N}{K}$ <sup>4</sup>. Due to a certain additive property, using the bandwidth expansion factor will be more convenient in the conference channel scenario. A bandwidth expansion factor  $\tau$  is said to be achievable if there exists a series of

<sup>4</sup>The bandwidth expansion factor terminology is motivated by the real time application where the bandwidth of the channel must be  $N/K$  times the bandwidth of the source process.

source-channel codes with  $N, K \rightarrow \infty$  but  $\frac{N}{K} \rightarrow \tau$ , such that  $P_e^{N,K} \rightarrow 0$ . In the feedback-relay and multicast channel, minimizing the bandwidth expansion factor reduces to the more conventional concept of maximizing the rate given by  $R = \frac{\log_2(M)}{N}$ , where  $M$  is the size of message set at the source node.

10) Throughout the sequel we will use the shorthand notation

$$C(x) = \frac{1}{2} \log(1 + x). \quad (7)$$

The three-node network model encompasses many important network communication scenarios with a wide range of complexity, controlled by various configurations of the index sets and the sources. From this perspective, the relay channel represents the simplest situation where one node serves as the relay for the other source-destination pair, e.g.,  $\mathcal{S}_2 = \mathcal{S}_3 = \phi$ ,  $I_1 = I_2 = \phi$  and  $I_3 = \{1\}$ . If we enlarge the index set  $I_2 = \{1\}$ , meaning node-2 now is also interested in obtaining the source message, then the problem becomes the multicast channel. Furthermore, if the two receivers (node-2 and 3) in the multicast case have additional observations, i.e.,  $S_2$  and  $S_3$ , which are correlated with the source variable  $S_1$ , then the problem generalizes to the so-called multicast with side information scenario. We refer to the most complex scenario as the conference channel. In this scenario, the three sources are correlated and every node attempts to reconstruct the other two sources, i.e.,  $I_i = \{1, 2, 3\} - \{i\}$ . While it is easy to envision other variants of the three node network, we decide to limit ourselves to these special cases. This choice stems from our belief that other scenarios do not add further insights to our framework. For example, another variant of the feedback-relay channel would allow the relay to observe its own side information. Careful consideration of this case, however, shows that our analysis in Section III extends to this case with only slight modifications. Similarly, inspired by our modular approach for the conference channel, one can decompose the multiple-access channel with correlated sources into two stages of feedback-relay channels with side information.

### III. THE FEEDBACK-RELAY CHANNEL

Our formulation for the three node network allows for a more realistic investigation of the relay channel with feedback. In this scenario, node-1 is designated as the source node, node-3 the destination, and node-2 the relay. Since there is only one source in this case, one can easily see that maximizing the achievable rate  $R$  from source to destination is equivalent to minimizing

the bandwidth expansion factor. Before proceeding to our scenario of interest, we review briefly the available results on the AWGN relay channel.

In a recent work [10], Kramer *et al.* present a comprehensive overview of existing cooperation strategies, and the corresponding achievable rates, for full-duplex/half-duplex relay channels. In our work, we focus on two classes of cooperation strategies, namely 1) Decode and Forward (DF) and 2) Compress and Forward (CF) strategies.<sup>5</sup>

In DF cooperation, the relay node first decodes the source message and then starts aiding the destination node in decoding (through a beamforming approach). More specifically, the transmission cycle is divided into two stages. In the first stage, which occupies a fraction  $t$  of the total time, the source node sends common messages to both the relay and destination node. Typically more information is sent in this stage than can the destination node decode. Having successfully decoded the source message in this stage, the relay node uses the second stage to help the destination resolve its uncertainty about the transmitted codeword. During the second stage, a new message is also sent to the destination node from the source node, along with the information from the relay. When the source-relay link is very noisy, one can argue that requiring the relay node to decode the message before starting to help the destination may, in fact, adversely affect performance. The CF strategy avoids this drawback by asking the relay to “compress” its observations and send it to the destination. In this approach, Wyner-Ziv source compression is employed by the relay to allow the destination node to obtain a (noisy) copy of the relay observations. Similar to the DF strategy, the transmission cycle is divided into two stages. During the first stage, both the relay and the destination listen to the source node. The relay then quantizes its observations and sends the quantized data to the destination node during the second stage. In general, the correlation between the relay observations and the destination observations can be exploited by the Wyner-Ziv coding to reduce the data rate at the relay node. During the second stage, new information is also sent by the source that further boosts the total throughput. Here we omit the detailed proofs and refer the interested readers to the relevant works [5], [7], [10], [11], [12], [13], [14], [21]. We note, however, that the statement of the results allows for employing optimal power allocation policies to maximize the throughput.

<sup>5</sup>For simplicity of presentation, in our notation, we do not distinguish between “partial” DF and “complete” DF strategies (The same applies to CF). For more details the reader is referred to [5].

*Lemma 1:* The achievable rate of the DF and CF strategies are given by

$$R_{DF} = \sup_{t, r_{12}, P_i^{(j)}} \min \left\{ tC\left(h_{12}^2 P\right) + (1-t)C\left((1-r_{12}^2)h_{13}^2 P_1^{(2)}\right); \right. \\ \left. tC\left(h_{13}^2 P\right) + (1-t)C\left(h_{13}^2 P_1^{(2)} + 2r_{12}h_{13}h_{23}\sqrt{P_1^{(2)}P_2^{(2)}} + h_{23}^2 P_2^{(2)}\right) \right\}. \quad (8)$$

$$R_{CF} = \sup_{t, P_i^{(j)}} tC\left(\left(h_{13}^2 + \frac{h_{12}^2}{1+\sigma_2^2}\right)P\right) + (1-t)C\left(h_{13}^2 P_1^{(2)}\right). \quad (9)$$

where

$$\sigma_2^2 = \frac{(h_{12}^2 + h_{13}^2)P + 1}{(h_{13}^2 P + 1) \left( \left(1 + \frac{h_{23}^2 P_2^{(2)}}{h_{13}^2 P_1^{(2)} + 1}\right)^{\frac{1-t}{t}} - 1 \right)}, \quad (10)$$

and

$$P_1^{(2)} + P_2^{(2)} = P. \quad (11)$$

We are now ready to present the cooperation strategy for the relay channel with feedback. In a nutshell, the proposed strategy combines the DF and CF strategies to overcome the bottleneck of a noisy source-relay channel. In this FeedBack (FB) approach, the destination first assists the relay in decoding via CF cooperation. After decoding, the relay starts helping the destination via a DF configuration. Due to the half-duplex constraint, every cycle of transmission is divided into the following three stages (as shown in Fig. 2).

- The first state lasts for a fraction  $\alpha t$  of the cycle ( $0 \leq t, \alpha \leq 1$ ). In this stage, both the relay and the destination listen to the source. We refer to the network state in this stage as  $m_1$ .
- The feedback stage lasts for a fraction  $(1-\alpha)t$  of the cycle. In this stage, the relay listens to both the destination and the source. Since the destination is not yet able to completely decode the source message, it sends to the relay node a Wyner-Ziv compressed version of its observations. We refer to the network state in this stage as  $m_3$ .
- The final stage lasts for a fraction  $(1-t)$  of the cycle. Having obtained source information, the relay is now able to help the destination node in decoding the source message. We refer to the network state in this stage as  $m_2$ .

The time-division parameters  $t$  and  $\alpha$  control the relative duration of each network state. In particular,  $t$  represents the total time when the relay node is in the receive mode. The feedback parameter  $\alpha$  controls the amount of feedback, i.e., a  $(1-\alpha)$  fraction of the total relay listening

time is dedicated to feedback. Here, we stress that this formulation for a relay channel with feedback represents a “realistic” view that attempts to capture the constraints imposed by the wireless scenario (as opposed to the *ideal* feedback assumed in existing works, e.g., [5]). The feedback considered here simply refers to transmission from the destination to relay over the same (noisy) wireless channel. Using random coding arguments we obtain the following achievable rate for the proposed feedback scheme.

*Lemma 2:* The achievable rate of the feedback scheme is given by

$$R_{FB} = \sup_{\alpha, t, r_{12}, P_i^{(j)}} \min \left\{ \alpha t C \left( \left( \frac{h_{13}^2}{1 + \sigma_3^2} + h_{12}^2 \right) P_1^{(1)} \right) + (1 - \alpha) t C \left( h_{12}^2 P_1^{(3)} \right) \right. \\ \left. + (1 - t) C \left( (1 - r_{12}^2) h_{13}^2 P_1^{(2)} \right); \right. \\ \left. \alpha t C \left( h_{13}^2 P_1^{(1)} \right) + (1 - t) C \left( h_{13}^2 P_1^{(2)} + 2r_{12} h_{13} h_{23} \sqrt{P_1^{(2)} P_2^{(2)}} + h_{23}^2 P_2^{(2)} \right) \right\} \quad (12)$$

where

$$\sigma_3^2 = \frac{(h_{12}^2 + h_{13}^2) P_1^{(1)} + 1}{(h_{12}^2 P_1^{(1)} + 1) \left( \left( 1 + \frac{h_{23}^2 P_3^{(3)}}{h_{12}^2 P_1^{(3)} + 1} \right)^{\frac{1-\alpha}{\alpha}} - 1 \right)} \quad (13)$$

and  $r_{12}$  is the correlation between  $X_1, X_2$  during state  $m_2$ . In the proposed strategy, the total power constraint specializes to

$$P_1^{(1)} = P, \quad P_1^{(2)} + P_2^{(2)} = P, \quad P_1^{(3)} + P_3^{(3)} = P. \quad (14)$$

*Proof:* Please refer to Appendix I.  $\square$

Armed with Lemmas 1 and 2, we can now contrast the performance of the DF, CF, and FB strategies. Our emphasis is to characterize the fundamental properties of the feedback scheme and quantify the gain offered by it under different assumptions on the channel gains and total power. The *relay-off* performance, i.e.,  $R_{ro} = C(h_{13}^2 P)$ , serves as a lower bound on the achievable rate. In fact, the relay-off benchmark can be viewed as a special case of the three cooperative schemes. For example, setting  $P_2^{(2)} = 0$  and  $t = 0$  effectively reduces both DF and CF strategies to the relay-off case. Therefore, one can conceptually describe the order of containment of various schemes as “relay-off  $\subset$  DF  $\subset$  FB” and “relay-off  $\subset$  CF”. As for the performance upper bounds, the cut-set bounds [5] give rise to 1) a multi-transmitter rate  $R_{(1,2)-3} = C((h_{13}^2 + h_{23}^2)P)$  corresponding to perfect cooperation between the source and relay nodes; and 2) a multi-receiver

rate  $R_{1-(2,3)} = C((h_{13}^2 + h_{12}^2)P)$  corresponding to perfect cooperation between the relay and destination nodes.

The achievable rate for the DF strategy, i.e.,  $R_{DF}$ , enjoys an intuitive geometric interpretation: each expression within the min operator is a linear segment in the parameter  $t \in [0, 1]$  (see (8)). Hence, the optimal time  $t$ , assuming the other variables remain fixed, can be simply determined by the intersection point of the two associated line segments, as illustrated in Fig. 3. On the other hand,  $R_{FB}$  and  $R_{CF}$  are characterized by more complicated expressions due to the dependency of  $\sigma_3^2$  and  $\sigma_2^2$  upon the time-division parameters. Our next result finds upper bounds on  $R_{FB}$  and  $R_{CF}$  which allow for the same simple line-crossing interpretation as  $R_{DF}$ .

*Lemma 3:* The achievable rate of the feedback scheme is upper bounded by

$$R_{FB} \leq \sup_{\alpha, t, r_{12}, P_i^{(j)}} \min \left\{ \alpha t C(h_{12}^2 P_1^{(1)}) + (1 - \alpha) t C(h_{12}^2 P_1^{(3)} + h_{23}^2 P_3^{(3)}) + (1 - t) C((1 - r_{12}^2) h_{13}^2 P_1^{(2)}); \right. \\ \left. \alpha t C(h_{13}^2 P_1^{(1)}) + (1 - t) C(h_{13}^2 P_1^{(2)} + 2r_{12} h_{13} h_{23} \sqrt{P_1^{(2)} P_2^{(2)}} + h_{23}^2 P_2^{(2)}) \right\}. \quad (15)$$

The achievable rate of compress-and-forward is bounded by

$$R_{CF} \leq \sup_{t, P_i^{(j)}} \min \left\{ t C(h_{13}^2 P_1^{(1)}) + (1 - t) C(h_{13}^2 P_1^{(2)} + h_{23}^2 P_2^{(2)}); \right. \\ \left. t C((h_{13}^2 + h_{12}^2) P_1^{(1)}) + (1 - t) C(h_{13}^2 P_1^{(2)}) \right\}. \quad (16)$$

*Proof:* Please refer to Appendix II.  $\square$

Interestingly, Fig. 3 encodes a great deal of information regarding the performance of the three schemes. For example, when  $h_{12}^2 \leq h_{13}^2$ , the intersection point corresponding to decode-forward would fall below the flat line  $C(h_{13}^2 P)$  associated with the relay-off rate. More rigorously, we have the following statement.

*Theorem 1:* 1) If  $h_{12}^2 \leq h_{13}^2$  then  $R_{DF} \leq R_{ro}$ .

2) If  $h_{23}^2 \leq h_{13}^2$  then  $R_{CF} \leq R_{ro}$ .

3) If  $h_{23}^2 \leq h_{12}^2$  then  $R_{FB} \leq R_{DF}$ .

*Proof:* Please refer to Appendix III.  $\square$

Theorem 1 reveals the fundamental impact of channel coefficients on the performance of the different cooperation strategies. In particular, the DF strategy is seen to work well with a

“strong” source-relay link. If, at the same time, the relay-destination link is stronger, then one may exploit feedback, i.e.,  $\alpha \neq 1$ , to improve performance. The next result demonstrates the asymptotic optimality of the feedback scheme in the limit of large  $h_{12}$  or  $h_{23}$ .

- Theorem 2:*
- 1) As  $h_{12}$  increases, both DF- and FB-scheme achieve the optimal beam-forming benchmark, while CF-scheme is limited by a sub-optimal rate  $C(\max\{h_{13}^2, h_{23}^2\}P)$ .
  - 2) As  $h_{23}$  increases, both CF- and FB-scheme achieve the optimal multi-receiver benchmark, while DF-scheme only approaches to a sub-optimal rate  $C(\max\{h_{12}^2, h_{13}^2\}P)$ .

The proof of Theorem 2 is a straightforward limit computation, and hence, is omitted for brevity. So far we have kept the total power  $P$  constant. But in fact, the achievable rate as a function of  $P$  offers another important dimension to the problem. First, we investigate the low power regime, which is greatly relevant to the wide-band scenario. In this case we study the slope  $S$  of the achievable rate with respect to  $P$  (i.e.,  $R \sim \frac{1}{2}(\log e)SP$ ). Note that the relay-off benchmark has a slope  $h_{13}^2$ .

*Theorem 3:* Let  $f_1(\theta, r_{12}, h_{13}, h_{23}) = h_{13}^2 \cos^2 \theta + 2r_{12}h_{13}h_{23} \cos \theta \sin \theta + h_{23}^2 \sin^2 \theta$  and  $f_2(\theta, r_{12}, h_{13}) = (1 - r_{12}^2)h_{13}^2 \cos^2 \theta$  be a shorthand notation, then

- 1) When  $h_{12}^2 \geq h_{13}^2$

$$S_{DF} = \max_{\theta, r_{12}} \frac{f_1(\theta, r_{12}, h_{13}, h_{23})h_{12}^2 - f_2(\theta, r_{12}, h_{13})h_{13}^2}{f_1(\theta, r_{12}, h_{13}, h_{23}) + h_{12}^2 - f_2(\theta, r_{12}, h_{13}) - h_{13}^2}, \quad (17)$$

and

$$\frac{(h_{13}^2 + h_{23}^2)h_{12}^2}{h_{23}^2 + h_{12}^2} \leq S_{DF} \leq \frac{(h_{13}^2 + h_{23}^2)h_{12}^2 - h_{13}^4}{h_{23}^2 + h_{12}^2 - h_{13}^2}. \quad (18)$$

- 2)  $S_{CF} = h_{13}^2$  with  $t_{opt} \rightarrow 1$ .
- 3)  $S_{FB} = S_{DF}$  with  $\alpha_{opt} \rightarrow 1$ .

*Proof:* Please refer to Appendix IV. □

It follows from Theorem 3 that given  $h_{12}^2 \geq h_{13}^2$ , DF cooperation delivers a larger slope than the relay-off, i.e.,

$$S_{DF} - h_{13}^2 \geq \frac{h_{23}^2(h_{12}^2 - h_{13}^2)}{h_{23}^2 + h_{12}^2} \geq 0. \quad (19)$$

However, CF cooperation does not yield any gain in the low power regime. Similarly, we see that the CF stage of the proposed FB becomes useless, and hence, the scheme reduces to the DF approach in the low power regime. The reason lies in the fact that for small  $P$ , the channel

output is dominated by the noise, and hence, the compression algorithm inevitably operates on the noise, resulting in diminishing gains.

We next quantify the SNR gain of the three schemes in the high power regime, that is, to characterize  $R \sim \frac{1}{2} \log P + \frac{1}{2}G$  as  $P \rightarrow \infty$ .

*Theorem 4:* Following the same shorthand notations as in Theorem 3, we obtain

1) Given  $h_{12}^2 \geq h_{13}^2$ ,

$$G_{DF} = \max_{\theta, r_{12}} \frac{\log f_1(\theta, r_{12}, h_{13}, h_{23}) \cdot \log h_{12}^2 - \log f_2(\theta, r_{12}, h_{13}) \cdot \log h_{13}^2}{\log [f_1(\theta, r_{12}, h_{13}, h_{23})h_{12}^2] - \log [f_2(\theta, r_{12}, h_{13})h_{13}^2]}. \quad (20)$$

2)

$$G_{CF} = \max_{t, \theta} t \log \left( h_{13}^2 + \frac{h_{12}^2}{1 + \sigma_2^2(\infty)} \right) + (1 - t) \log (h_{13}^2 \cos^2 \theta) \quad (21)$$

where

$$\sigma_2^2(\infty) = \frac{h_{12}^2 + h_{13}^2}{h_{13}^2 \left( \left( 1 + \frac{h_{23}^2}{h_{13}^2} \tan^2 \theta \right)^{\frac{1-t}{t}} - 1 \right)}. \quad (22)$$

3)  $G_{FB} = G_{DF}$  with  $\alpha_{opt} \rightarrow 1$ .

*Proof:* Please refer to Appendix V. □

Theorem 4 reveals the fact that strict feedback ( $\alpha \neq 1$ ) does not yield a gain in high power regime. The reason for this behavior can be traced back to the half-duplex constraint. When  $\alpha \neq 1$ , the destination spends a fraction  $(1 - \alpha)t$  of time transmitting to the relay, which cuts off the time in which it would have been listening to the source in non-feedback schemes. Such a time loss reduces the pre-log constant, which cannot be compensated by the cooperative gain when P becomes large.

At this point, we wish to make a side comment contrasting the half-duplex constraint with orthogonal relay channels. The orthogonal cooperation framework was recently proposed as a practical way to address the half-duplex requirement [7], [18]. For simplicity, let's consider the non-feedback scenario and assume that the available bandwidth is  $W$  Hz, and hence, the total resources available to every node in network is  $2W$  real dimensions per second. The half-duplex constraint dictates **only** orthogonality at each node, where the available degrees of freedom, in the time-frequency plane, is splitted into two parts. The node uses the first part to receive and the second to transmit. In the orthogonal cooperation approach, however, one imposes orthogonality at the network level (i.e., no two nodes can now transmit in the same degree of freedom). In particular, the channel is split into two sub channels (either in time domain [18] or frequency

domain [7]), where the source uses one of the sub-channels to transmit information to the relay and destination, and the relay uses the other sub-channel to transmit to the destination. One can now see that this orthogonalization is sufficient but **not** necessary to satisfy the half-duplex constraint. Figure 4 shows the orthogonal cooperation scheme which splits the channel in the time domain. When relay sends, it can use either the DF or CF strategies. Using the same argument as in the previous part, one obtains the following achievable rate for the orthogonal DF strategy scheme,

$$R_{ODF} = \max_t \min\{tC(h_{12}^2 P); tC(h_{13}^2 P) + (1-t)C(h_{23}^2 P)\}. \quad (23)$$

It is now clear that  $R_{ODF}$  is just a special case of  $R_{DF}$  where, for any  $t$ , one can obtain the corresponding  $R_{ODF}$  by setting  $P_1^{(2)} = 0$  in (8). One can use the fact that  $P_1^{(2)} = 0$  is not necessarily the optimal power assignment that maximizes (8) to argue for the sub-optimality of the orthogonal DF strategy (i.e.,  $R_{DF} \geq R_{ODF}$ ). More generally, the same argument can be used to establish the sub-optimality of any orthogonal cooperation strategy.

We conclude this section with simulation results that validate our theoretical analysis. Figure 5 reports the achievable rate of various schemes, when  $h_{12} = 1.8$ ,  $h_{13} = 1$ , and  $h_{23} = 200$ . This corresponds to the case when the source-relay channel is a little better than the source-destination channel, and the relay-destination channel is quite good. This is the typical scenario when feedback results in a significant gain, as demonstrated in the figure. In the figure, we also see the sub-optimality of orthogonal cooperation strategies. Figure 6 reports the achievable rates of various schemes, when  $h_{12} = 1.8$ ,  $h_{13} = 1$ , and  $P = 1$ , as we vary the relay-destination channel gain  $h_{23}$ . We can see that as the relay-destination channel becomes better, the advantage of feedback increases. Figures 7, 8, 9 illustrate regions in the  $h_{12}$ – $h_{23}$  plane ( $h_{13} = 1$ ) corresponding to the best of the three strategies. It is seen that feedback can improve upon both DF and CF strategies in certain operating regions. However, as predicted by our analysis, such gain diminishes when either  $P \rightarrow 0$  or  $P \rightarrow \infty$ . Overall, we can see that the proposed FB cooperation scheme combines the benefits of both the DF and CF cooperation strategies, and hence, attains the union of the “nice” properties of the two strategies. On the other hand, the gain offered by feedback seems to be limited to certain operating regions, as defined by the channel gains, and diminishes in either the low or high power regime.

#### IV. THE MULTICAST CHANNEL

The relay channel, considered in the previous section, represents the simplest example of a three-node wireless network. A more sophisticated example can be obtained by requiring node-2 to decode the message generated at node-1. This corresponds to the multicast scenario. Similar to the relay scenario, we focus on maximizing the achievable rate from node-1 to both node-2 and 3, without any loss of generality. The half-duplex and total power constraints, adopted here, introduce an interesting design challenge. To illustrate the idea, suppose node-2 decides to help node-3 in decoding. In this case, not only does node-2 compete with the source node for transmit power, but it also sacrifices its listening time for the sake of helping node-3. It is, therefore, not clear *a-priori* if the network would benefit from this cooperation. In the following, we answer this question in the affirmative and further propose a greedy cooperation strategy that enjoys several *nice* properties.

In a recent work [16], the authors considered another variant of the multicast channel and established the benefits of receiver cooperation in this setup. The fundamental difference between the two scenarios is that, in [16], the authors assumed the existence of a dedicated link between the two receivers. This dedicated link was used by the *strong* receiver to help the *weak* receiver in decoding through a DF strategy. As expected, such a cooperation strategy was shown to strictly enlarge the achievable rate region [16]. In our work, we consider a more representative model of the wireless network in which all communications take place over the same channel, subject to the half-duplex and total power constraints. Despite these constraining assumptions, we still demonstrate the significant gains offered by receiver cooperation. Inspired by the feedback-relay channel, we further construct a greedy cooperation strategy that significantly outperforms the DF scheme [16] in many relevant scenarios.

In the non-cooperative scenario, both node-2 and node-3 will listen all the time, and hence, the achievable rate is given by

$$C_{non-coop} = C(\min\{h_{12}^2, h_{13}^2\}P). \quad (24)$$

Due to the half-duplex constraint, time is valuable to both nodes, which makes them selfish and unwilling to help each other. Careful consideration, however, reveals that such a *greedy* approach will lead the nodes to cooperate. The enabling observation stems from the feedback strategy proposed for the relay channel in which the destination was found to get a higher

achievable rate if it sacrifices some of its receiving time to help the relay. Motivated by this observation, our strategy decomposes into three stages, without loss of generality we assume  $h_{12}^2 > h_{13}^2$ , 1)  $m_1$  lasting for a fraction  $\alpha t$  of the frame during which both receivers listen to node-1; 2)  $m_3$  occupying  $(1-\alpha)t$  fraction of the frame during which node-3 sends its compressed signal to node-2; and 3)  $m_2$  (the rest  $1-t$  fraction) during which node-1 and 2 help node-3 finish decoding. One major difference between the multicast and relay scenarios is that in the second stage the source cannot send additional (new) information to node-3, for it would not be decoded by node-2, thus violating the multicast requirement that both receivers obtain the same source information. Here, we observe that the last stage of cooperation, in which node-2 is helping node-3, is still motivated by the greedy approach. The idea is that node-1 will continue transmitting the same codeword until both receivers can successfully decode. It is, therefore, beneficial for node-2 to help node-3 in decoding faster to allow the source to move on to the next packet in the queue. A slight modification of the proof of Lemma 2 results in the following.

*Lemma 4:* The achievable rate of the greedy strategy based multicast scheme is given by

$$R_g = \sup_{\alpha, t, P_i^{(j)}} \min \left\{ \alpha t C \left( \left( \frac{h_{13}^2}{1 + \sigma_4^2} + h_{12}^2 \right) P \right) + (1 - \alpha) t C \left( h_{12}^2 P_1^{(3)} \right); \right. \\ \left. \alpha t C \left( h_{13}^2 P \right) + (1 - t) C \left( (h_{13}^2 + h_{23}^2) P \right) \right\} \quad (25)$$

where

$$\sigma_4^2 = \frac{(h_{12}^2 + h_{13}^2)P + 1}{(h_{12}^2 P + 1) \left( \left( 1 + \frac{h_{23}^2 P_3^{(3)}}{h_{12}^2 P_1^{(3)} + 1} \right)^{\frac{1-\alpha}{\alpha}} - 1 \right)}, \quad (26)$$

and  $r_{12}$  denotes the correlation between  $X_1, X_2$  during state  $m_2$ . The ‘‘sup’’ operator is taken over the total power constraint.

We observe that the DF multicast scheme corresponds to the special case of  $\alpha = 1$ , which has a rate

$$R_{DF} = \sup_t \min \left\{ t C(h_{12}^2 P); t C(h_{13}^2 P) + (1 - t) C((h_{13}^2 + h_{23}^2) P) \right\}. \quad (27)$$

The cut-set upperbounds give rise to the two following benchmarks: beam-forming  $R_{(1,2)-3} = C((h_{13}^2 + h_{23}^2)P)$  and multi-receiver  $R_{1-(2,3)} = C((h_{13}^2 + h_{12}^2)P)$ . Similar to the relay channel scenario, we examine in the following the asymptotic behavior of the greedy strategy as a function of the channel coefficients and available power.

*Theorem 5:* 1) The greedy cooperative multicast scheme strictly increases the multicast achievable rate (as compared to the non-cooperative scenario).

2) The greedy strategy approaches the beam-forming benchmark as  $h_{12}$  increases, i.e.,

$$\lim_{h_{12} \rightarrow \infty} R_g = C((h_{13}^2 + h_{23}^2)P). \quad (28)$$

3) The greedy strategy approaches the multi-receiver benchmark as  $h_{23}$  increases, i.e.,

$$\lim_{h_{23} \rightarrow \infty} R_g = C((h_{12}^2 + h_{13}^2)P). \quad (29)$$

4) As  $P \rightarrow 0$ , the slope of the greedy strategy achievable rate is given by

$$S_g = \frac{h_{12}^2(h_{23}^2 + h_{13}^2)}{h_{12}^2 + h_{23}^2}. \quad (30)$$

5) As  $P \rightarrow \infty$ , the SNR gain  $G_g = G_{non-coop} = \log h_{13}^2$  with  $t_{opt} \rightarrow 1$ .

*Proof:* Please refer to Appendix VI. □

Parts 2), 3) demonstrate the asymptotic optimality of the greedy multicast as the channel gains increase (the proof follows the same line as that of Theorem 2). On the other hand, we see that the large-power asymptotic of the multicast channel differs significantly from that of the relay channel. In the relay case (Theorem 4), the contribution of feedback diminishes ( $G_{FB} = G_{DF}$ ) in this asymptotic scenario, but cooperation was found to be still beneficial, that is  $G_{DF} > \log h_{13}^2$ . To the contrast, the gain of receiver cooperation in the multicast channel disappears as  $P$  increases. This is because, unlike the relay scenario, at least one receiver must cut its listening time in any cooperative multicast scheme due to the half-duplex constraint. Such a reduction induces a pre-log penalty in the rate, which results in substantial loss that cannot be compensated by cooperation as  $P \rightarrow \infty$ , and hence, the greedy strategy reduces to the non-cooperative mode automatically.

Figure 10 compares the achievable rate of the various multicast schemes where the DF cooperation strategy is shown to outperform the non-cooperation scheme. It is also shown that optimizing the parameter  $\alpha$  provides an additional gain (Note  $R_{DF}$  in the figure corresponds to  $\alpha = 1$ ). Figure 11 reports the achievable rate of the three schemes when  $h_{12} = h_{13}$ . In this case, it is easy to see that DF strategy yields **exactly** the same performance as the non-cooperative strategy. On the other hand, as illustrated in the figure, the proposed greedy strategy is still able to offer a sizable gain. Figure 12 illustrates the fact that the gain of greedy strategy increases as  $h_{23}$  increases. The non-cooperation scheme is not able to exploit the inter-receiver channel,

and hence, its achievable rate corresponds to a flat line. The DF scheme can benefit from the inter-receiver channel, but its maximum rate is limited by  $C(h_{12}^2 P)$ , whereas the greedy strategy achieves a rate  $R_g = C((h_{12}^2 + h_{13}^2)P)$  as  $h_{23} \rightarrow \infty$ .

## V. THE CONFERENCE CHANNEL

Arguably the most demanding instantiation of the three-node network is the conference channel. Here, the three nodes are assumed to observe correlated data streams and every node is interested in communicating its observations to the other two nodes. In a first step to understand this channel, one is naturally led to applying cut-set arguments to obtain a lower bound on the necessary bandwidth expansion factor<sup>6</sup>. To satisfy the conference channel requirements, every node needs to transmit its message to the other two nodes and receive their messages from them. Due to the half duplex constraint, these two tasks cannot be completed simultaneously. Take node-1 as an example and consider the transmission of a block of observations  $S_1^K$  to the other two nodes using  $N_t$  channel uses. To obtain a lower bound on the bandwidth expansion factor, we assume that node-2 and node-3 can fully cooperate, from a joint source-channel coding perspective, which converts the problem into a point-to-point situation. Then node-1 only needs to randomly divide its source sequences into  $2^{KH(S_1|S_2, S_3)}$  bins and transmit the corresponding bin index. With  $N_t$  channel uses, the information rate is  $\frac{KH(S_1|S_2, S_3)}{N_t}$ . The channel capacity between node-1 and the multi-antenna node-2, 3 is  $C((h_{12}^2 + h_{13}^2)P)$ . In order to decode  $S_1^K$  at node-2, 3 with a vanishingly small error probability, the following condition must be satisfied,

$$\frac{KH(S_1|S_2, S_3)}{N_t} \leq C((h_{12}^2 + h_{13}^2)P).$$

Similarly, with full cooperation between node-2 and node-3, the following condition is needed to ensure the decoding of the sequence  $S_2^K, S_3^K$  at node-1 with a vanishingly small error probability,

$$\frac{KH(S_2, S_3|S_1)}{N_r} \leq C((h_{12}^2 + h_{13}^2)P).$$

These two genie-aided bounds at node-1 imply that the minimum bandwidth expansion factor required for node-1 is  $\tau_{1,gen} = \frac{H(S_1|S_2, S_3) + H(S_2, S_3|S_1)}{C((h_{12}^2 + h_{13}^2)P)}$ . Similarly, we can obtain the corresponding genie-aided bounds for node-2 and node-3,  $\tau_{2,gen} = \frac{H(S_2|S_1, S_3) + H(S_1, S_3|S_2)}{C((h_{12}^2 + h_{23}^2)P)}$ ,  $\tau_{3,gen} =$

<sup>6</sup>Here, we use the bandwidth expansion factor, instead of the achievable rate, since it enjoys a nice additive property that will simplify the development.

$\frac{H(S_3|S_1, S_2) + H(S_1, S_2|S_3)}{C((h_{13}^2 + h_{23}^2)P)}$ . To satisfy the requirement for all these three nodes, the minimum bandwidth expansion factor for this half-duplex conference channel is therefore

$$\tau_{gen} \geq \max_{i=1,2,3} \tau_{i,gen}. \quad (31)$$

At this point, we remark that it is not clear whether the genie-aided bound in (31) is achievable. Moreover, finding the optimal cooperation strategy for the conference channel remains an elusive task<sup>7</sup>. However, inspired by our greedy multicast strategy, we propose in the following a modular cooperation approach composed of three *cooperative multicast with side information* stages. In this scheme, each node takes a turn to multicast its information to the other two nodes. The multicast problem here is more challenging than the scenario considered in Section IV due to the presence of correlated, and different, side information at the two receive nodes. As argued in the following section, in order to fully exploit this side information, one must adopt a cooperative source-channel coding approach in every multicast stage. Furthermore, from one stage to the next, the side-information available at the different nodes changes. For instance, assuming the first stage is assigned to node-1, then the side-information available at node-2 and 3 will enlarge after the first stage to  $(S_1, S_2)$  and  $(S_1, S_3)$ , respectively. Now, suppose node-2 is scheduled to multicast next, then the rate required by node-3 is now reduced to  $H(S_2|S_1, S_3)$ , thanks to the additional side-information  $S_1$ . Thus, one can see that the overall performance depends on the efficiency of the scheduling algorithm. In Section V-B, we present a greedy scheduling algorithm that enjoys a low computational complexity and still achieves a near-optimal performance.

#### A. Multicast with Side-information

The relay and multicast scenarios considered previously share the common feature of the presence of only one source  $S_1$ . Here, we expand our investigation of the multicast scenario by allowing the receive nodes to observe correlated, and possibly different, side information. To simplify the presentation, without sacrificing any generality, we assume that node-1 is the source and node-2 and 3 are provided with the side information  $S_2$  and  $S_3$ , respectively. Before presenting our greedy cooperation strategy, we study the non-cooperative scenario where the two receive nodes are not allowed to communicate. This investigation yields an upper bound on the bandwidth expansion factor achievable through cooperation.

<sup>7</sup>Most of the earlier works on the conference channel has focused on the source coding aspect, e.g., [17].

One can obtain a simple-minded transmission scheme by separating the source and channel coding components. In this approach, by appealing to the standard random binning argument [17], node-1 encodes the source sequence at the rate  $\max\{H(S_1|S_2), H(S_1|S_3)\}$  which allows both receivers to decode with the aid of their side-information. Such a source code is then sent via the multicast channel assuming no receiver cooperation, which corresponds to a transmission rate  $\min\{C(h_{12}^2P), C(h_{13}^2P)\}$ . Therefore, the above scheme would require

$$\tau = \frac{\max\{H(S_1|S_2), H(S_1|S_3)\}}{\min\{C(h_{12}^2P), C(h_{13}^2P)\}} \quad (32)$$

channel uses per source symbol. In (32), the source code based on random binning reflects the worst-case scenario corresponding to the least correlated receiver node, i.e.,  $\max\{H(S_1|S_2), H(S_1|S_3)\}$ . A more efficient solution utilizes a *nested binning* approach that combines the information required by the two receive nodes into a single hierarchical binning scheme. For the convenience of exposition, we assume that  $H(S_1|S_2) > H(S_1|S_3)$ . A source sequence  $s_1^K$  is randomly assigned to one of  $2^{KH(S_1|S_2)}$  bins. This is the low-level indexing sufficient for node-2 to decode with side-information  $S_2$ . These indices are then (randomly) divided into  $2^{KH(S_1|S_3)}$  equal-sized groups, which corresponds to the random binning approach for node-3. Therefore, a source sequence  $s_1^K$  is associated with an index-pair  $(b, c)$ , where  $b \in [1, 2^{KH(S_1|S_3)}]$  is the group index and  $c \in [1, 2^{K(H(S_1|S_2)-H(S_1|S_3))}]$  identifies the bin index within a group. Given side-information  $S_3$  (more correlated with the source), node-3 needs only the group index  $b$  to recover the source sequence. But the low-level bin index is necessary for node-2 to decode. In summary, the above nested binning scheme permits the source node to send  $(b, c)$  to node-2 while only  $b$  to node-3. Such a structured message is called the *degraded information set* in [15] where  $b$  is the “common” information for both receivers and  $c$  the “private” information required by only one of the two receivers. The corresponding rate set can be written as  $(R_2, 0, R_0)$ , where  $R_2$  is the rate associated with the private message for node-2,  $R_0$  is the rate associated with the common message, and node-3 receives no private information. This broadcast channel with a degraded message set has been studied in [15] (and references therein).

*Theorem 6 (see [15]):* The capacity region of broadcast with degraded information set is the

convex hull of the closure of all  $(R_2, 0, R_0)$  satisfying

$$\begin{aligned} R_2 &\leq I(X_1; Y_2|U), \\ R_0 &\leq I(U; Y_3), \\ R_2 + R_0 &\leq I(X_1; Y_2), \end{aligned} \tag{33}$$

for some joint distribution  $p(u)p(x_1|u)p(y_2, y_3|x_1)$ .

If the broadcast channel itself is degraded then the above three constraints can be simplified [15]. Consider the case where  $X_1 \rightarrow Y_3 \rightarrow Y_2$  forms a Markov chain. If the last constraint is satisfied (in which case node-2 can decode both the private and common message), node-3 can also decode both parts of the source message although it does not need the private part. On the other hand, if  $X_1 \rightarrow Y_2 \rightarrow Y_3$ , the problem can be reduced to the conventional (degraded) broadcast setting where the rate  $R_2/R_0$  is for node-2/3 and node-2 would automatically decode the message for the degraded node-3. So, in this case, only the first two constraints are sufficient. The final step, in this approach, is to combine Theorem 6 with our nested binning approach. In this case, the rate set is given by  $R_2 = \frac{K(H(S_1|S_2)-H(S_1|S_3))}{N}$  and  $R_0 = \frac{KH(S_1|S_3)}{N}$  and we obtain the following result.

*Lemma 5:* For multicast with side-information, the achievable bandwidth expansion factor  $\tau = N/K$  based on nested binning source coding and degraded information set broadcasting is given by

1) if  $h_{12}^2 < h_{13}^2$ ,

$$H(S_1|S_2) \leq \tau C(h_{12}^2 P). \tag{34}$$

2) if  $h_{12}^2 > h_{13}^2$ ,

$$\begin{aligned} H(S_1|S_2) - H(S_1|S_3) &\leq \tau C\left(\gamma h_{12}^2 P\right), \\ H(S_1|S_3) &\leq \tau C\left(\frac{(1-\gamma)h_{13}^2 P}{1+\gamma h_{13}^2 P}\right). \end{aligned} \tag{35}$$

for some  $\gamma$ .

Now, we are ready to describe our greedy cooperative source-channel coding approach. Similar to the multicast scenario, the receive nodes follow a greedy strategy to determine the order of decoding. Due to the presence of side information, however, a more careful approach must be employed in choosing the *strong* receiver. To illustrate the idea, consider the following degenerate

case, where  $S_3$  is independent of  $S_1$ ,  $S_1 = S_2$ , and  $h_{12}^2 < h_{13}^2$ . Although the channel between node-1 and node-2 is worse in this case, node-2 knows the information  $S_1^K$  from the beginning because  $S_1 = S_2$ . So it can start to cooperate with node-1 from the very beginning. This toy example suggests that one should take the amount of side information available at each node into consideration. In our scheme, each node calculates the expected bandwidth expansion factor assuming no receiver cooperation,  $\tau_{ex,i} = H(S_1|S_i)/C_i$ , where  $C_i$  denotes the link capacity  $C(h_{1i}^2P)$ . The receive node with the smaller  $\tau_{ex}$  is deemed as the *strong* node, and hence, will decode first. Our definition of strong and weak highlights the cooperative source-channel coding approach proposed in this paper. Without loss of generality, we assume  $\tau_{ex,2} < \tau_{ex,3}$ . However, the “weak” node-3 may still decide to assist node-2 in decoding through a CF approach, in a way similar to Section IV, hoping to benefit from node-2’s help after it decodes. After node-2 successfully decoding, with/without the additional help from node-3, it coordinates with the source node to facilitate decoding at node-3, in order to start the next round of multicast.

To better describe the cooperative source-channel coding, we consider first the simple case where node-3 does not help node-2. We randomly bin the sequences  $S_1^K$  into  $2^{KH(S_1|S_2)}$  bins and denote the bin index by  $w \in [1, 2^{KH(S_1|S_2)}]$ . We further denote by  $f_{s_1}$  the mapping function  $w = f_{s_1}(s_1^K)$ . We then independently generate another bin index  $b$  for every sequence  $S_1^K$  by picking  $b$  uniformly from  $\{1, 2, \dots, 2^{KR}\}$ , where  $R$  is to be determined later. Let  $B(b)$  be the set of all sequences  $S_1^K$  allocated to bin  $b$ . Thus, every source sequence has two bin indices  $\{w, b\}$  associated with it. A full cooperation cycle is divided into two stages, where we refer to the network state in these two stages as  $m_1$  and  $m_2$ , respectively. In the first stage using for  $N_1$  channel uses, node-1 sends the message  $w$  to node-2 using a capacity achieving code. This stage is assumed to last for  $N_1$  channel uses. At the end of this state, node-2 can get a reliable estimate  $\hat{w} = w$  if the condition  $KH(S_1|S_2) \leq N_1C(h_{12}^2P)$  is satisfied. Next, node-2 searches in the bin specified by  $\hat{w}$  for the one and only one  $\hat{s}_{21}^K$  that is typical with  $s_2^K$ . If none exists, decoding error is declared, otherwise,  $\hat{s}_{21}^K$  is the decoding sequence. During this stage, node-3 computes a list  $\ell(\mathbf{y}_{3,m_1})$  such that if  $w' \in \ell(\mathbf{y}_{3,m_1})$  then  $\{\mathbf{x}_{1,m_1}(w'), \mathbf{y}_{3,m_1}\}$  are jointly typical. A key point of our scheme is that node-3 does not attempt to decode  $w$ , but rather proceeds to decoding  $s_1^K$  directly. After node-2 decodes  $s_1^K$  correctly, it knows the pair  $\{w, b\}$ , and hence, in the second stage node-2 and node-1 cooperate to send the message  $b$  to node-3. At the end this stage, if the parameters are appropriately chosen, node-3 can decode  $b$  correctly. Node-3 then

searches in the bin  $B(b)$  for the one and only one  $\hat{s}_{31}^K$  that is jointly typical with  $s_3^K$  and that  $f_{s1}(\hat{s}_{31}^K) \in \ell(\mathbf{y}_{3,m_1})$ .

*Lemma 6:* With the proposed scheme, both node-2, 3 can decode  $S_1^K$  with a vanishingly small probability of error if  $\tau_0 = N_0/K, \tau_1 = N_1/K$  satisfy the following conditions

$$\begin{aligned} H(S_1|S_2) &\leq \tau_1 C(h_{12}^2 P), \\ H(S_1|S_3) - \frac{\min\{C(h_{13}^2 P), C(h_{12}^2 P)\} H(S_1|S_2)}{C(h_{12}^2 P)} &\leq \tau_0 C((h_{13}^2 + h_{23}^2) P). \end{aligned} \quad (36)$$

*Proof:* Please refer to Appendix VII.  $\square$

Next, we allow for the weak node-3 to assist the strong node-2 in decoding. The original  $N_1$  channel uses now split into two parts: 1) state  $m_1$  occupying  $\alpha N_1$  channel uses during which both receiver nodes listen to the source node; and 2) state  $m_3$  of the remaining  $(1 - \alpha)N_1$  channel uses during which node-3 sends a compressed received signal to node-2. At the end of the  $N_1$  network uses, node-2 decodes the source sequence and then proceeds to facilitate the same list-decoding at the other receiver as described above. The simple case where node-3 does not assist node-2 can be regarded as a special case of the greedy scheme when  $\alpha = 1$ . Slightly modifying the proof of Lemma 6, we obtain

*Lemma 7:* If  $\tau_0, \tau_1$  satisfy the following conditions, both node-2, 3 will decode  $S_1^K$  with vanishingly small probability of error.

$$\begin{aligned} H(S_1|S_2) &\leq \tau_1 R_{CF2}(\alpha), \\ H(S_1|S_3) - \frac{\alpha \min\{I(X_1; Y_3|m_1); I(X_1; \hat{Y}_3, Y_2|m_1)\} H(S_1|S_2)}{R_{CF2}(\alpha)} &\leq \tau_0 C((h_{13}^2 + h_{23}^2) P). \end{aligned} \quad (37)$$

Where  $R_{CF2}(\alpha)$  is the achievable rate of compress-forward scheme for the following relay channel: node-1 acts as the source, node-3 the relay that spends  $1 - \alpha$  part of the time in helping destination using CF scheme, and node-2 the destination. The symbol  $\hat{Y}_3$  stands for the compressed version of the received signal at node-3 ( $Y_3$ ).

Unfortunately, the expressions for the achievable bandwidth expansion factors do not seem to allow for further analytical manipulation. In order to shed more light on the relative performance of the different schemes, we introduce the *minimum energy per source observation* metric. Given the total transmission power  $P$ , the bandwidth expansion factor  $\tau$  translates to the energy requirement per source observation as

$$E(P) = \tau(P)P = \frac{N(P)P}{K}. \quad (38)$$

Let  $E_1(P)$  denotes the energy per source symbol for the benchmark based on broadcast with a degraded information set and  $E_2(P)$  for the proposed cooperative multicast scheme. It is easy to see that both  $E_1(P)$  and  $E_2(P)$  are non-increasing function of  $P$ , and hence, approach their minimal values as  $P \rightarrow 0$ , that is

$$E_{i,m} = \lim_{P \rightarrow 0} E_i(P) \text{ for } i \in \{1, 2\}. \quad (39)$$

Under the assumption that  $\tau_{ex,2} < \tau_{ex,3}$  and using Lemmas 5 and 7, one obtain:

*Theorem 7:* 1) Broadcast with degraded information set:

When  $H(S_1|S_2) > H(S_1|S_3)$ ,

$$E_{1,m} = \frac{2}{\log e} \left( \frac{H(S_1|S_2)}{h_{12}^2} + \left( \frac{1}{h_{13}^2} - \frac{1}{h_{12}^2} \right)^+ H(S_1|S_3) \right). \quad (40)$$

When  $H(S_1|S_3) > H(S_1|S_2)$ ,

$$E_{1,m} = \frac{2}{\log e} \left( \frac{H(S_1|S_3)}{h_{13}^2} + \left( \frac{1}{h_{12}^2} - \frac{1}{h_{13}^2} \right)^+ H(S_1|S_2) \right). \quad (41)$$

Here  $x^+ = \max\{x, 0\}$ .

2) Greedy strategy:

$$E_{2,m} = \frac{2}{\log e} \left( \frac{H(S_1|S_2)}{h_{12}^2} + \frac{h_{12}^2 H(S_1|S_3) - \min\{h_{13}^2, h_{12}^2\} H(S_1|S_2)}{(h_{13}^2 + h_{23}^2) h_{12}^2} \right). \quad (42)$$

3)  $E_{2,m} < E_{1,m}$ .

*Proof:* Please refer to Appendix VIII.  $\square$

In general, Theorem 7 reveals the dependence of the minimum energy per source observation for the two schemes on the correlation among the source variables and the channel gains. However, Theorem 7 also establishes the superiority of the cooperative source-channel coding over the non-cooperative benchmark in the general case (at least with respect to the minimum energy requirement). Thus, when combined with the results in Section IV, this result argues strongly for receiver cooperation in the multicast scenario even under the stringent half-duplex and total power constraints. Finally, Figures 14 and 15 validate our theoretical claims. Fig. 14 reports the relationship between power and bandwidth expansion factor, whereas Fig. 15 reports the relationship between power and energy per source observation for various schemes. In both figures, the gain offered by the proposed cooperative multicast scheme is evident.

### B. Multicast scheduler

The second step in the proposed solution for the conference channel is the design of the scheduler. As argued earlier, the efficiency of the scheduler has a critical impact on the overall performance. Given a specific multicast order, one can compute the overall bandwidth expansion factor by adding up the required  $\tau$  for every multicast stage. The *optimal* scheduler will choose the multicast order corresponding to the minimum bandwidth expansion factor among all possible permutations. The following result argues for the efficiency of our proposed cooperation scheme for the conference channel.

*Theorem 8:* The cooperative source-channel coding multicast scheme with the optimal scheduler has the following properties (in the conference channel):

- 1) It is asymptotically optimal, i.e., achieves the genie-aided bound, when any one of the channel coefficients is sufficiently large.
- 2) It always outperforms the broadcast with a degraded set based multicast scheme with the optimal scheduler.

*Proof:* Please refer to Appendix IX. □

One can argue, however, that the optimal scheduler suffers from a high computation complexity since every node is required to compute the overall bandwidth expansion factors for the six possible scheduling alternatives. To reduce the computational complexity, one can adopt the following greedy strategy. At the beginning of every multicast stage, every node that has not finished multicasting yet will calculate its expected bandwidth expansion factor based on the cooperative scheme for multicast with side-information. The greedy scheduler chooses the node with the least expected bandwidth expansion factor to transmit at this stage. After this node finishes and the side-information is updated, the scheduler computes the expected bandwidth expansion factor for the rest of nodes and selects the one with the least bandwidth expansion factor to multicast next. As a side comment, we note here that this approach is easily scalable for networks with more than three nodes. In general, this greedy scheduler constitutes a potential source for further sub-optimality. However, it can achieve the genie-aided bound in the asymptotic limit when one of the channel gains is sufficiently large. Take  $h_{23} \rightarrow \infty$  as an example. In this case, if one of the following conditions is satisfied, the greedy scheduler achieves the genie-aided bound:

- 1)  $H(S_2|S_1) < \min\{H(S_1|S_2), H(S_1|S_3), H(S_3|S_1)\}$  and  $H(S_3|S_1, S_2) < H(S_1|S_2, S_3)$ ,
- 2)  $H(S_3|S_1) < \min\{H(S_1|S_2), H(S_1|S_3), H(S_2|S_1)\}$  and  $H(S_2|S_1, S_3) < H(S_1|S_2, S_3)$ .

One can easily check that if 1) is satisfied, the greedy scheduler will choose the sequence  $2 \rightarrow 3 \rightarrow 1$  as the multicast order, which is the optimal order that achieves the genie-aided bound. If 2) is satisfied, the greedy scheduler will choose the sequence  $3 \rightarrow 2 \rightarrow 1$  as the multicast order, which is also the order that achieves the genie-aided bound in this case.

The numerical results in Figures 16 and 17 validate our claims on the efficiency of the proposed cooperation strategy. These figures compare the minimum energy required per source observation by each scheme, under randomly generated channel gains and correlation patterns. For each realization, we use numerical methods to find the optimal order and greedy order for cooperative scheme, and the corresponding minimum energy required per source observation, namely  $E_{oc}, E_{gc}$ . We also find the optimal order for the non-cooperative scheme and the corresponding minimum energy required per source observation  $E_{nc}$ . The minimum energy required per source observation by the genie-aided bound  $E_{gen}$  is used as a benchmark. In particular, for each realization, we calculate the ratio of the minimum energy required by the three schemes to the genie aided bound. We repeat the experiment 100000 times and report the histogram of the ratios in the figures. In Fig. 16, we see that 94 percent of the time, the proposed cooperative scheme with the greedy scheduler operates within 3 dB of the genie-aided bound. We also see that the performance of greedy scheduler is almost identical to the optimal scheduler. Figure 17 shows that the non-cooperative scheme operates more than 3 dB away from the genie-aided bound for 90 percent of the time. Moreover, there is a non-negligible probability, i.e., 8 percent, that this scheme operates 100 dB away from genie aided bound. It is clear that receiver cooperation reduces this probability significantly.

## VI. CONCLUSIONS

We have adopted a formulation of the three-node wireless network based on the half-duplex and total power constraints. We argued that this formulation unifies many of the special cases considered in the literature and highlights their structural similarities. In particular, we have proposed a greedy cooperation strategy in which the *weak* receiver first helps the *strong* receiver to decode in a CF configuration. After successfully decoding, the strong user starts assisting the weak user in a DF configuration. We have shown that different instantiations of this strategy

yield excellent performance in the relay channel with feedback, multicast channel, and conference channel. Our analysis for the achievable rates in such special cases sheds light on the value of feedback in relay channel and the need for a cooperative source-channel coding approach to efficiently exploit receiver side information in the wireless setting.

Extending our work to networks with arbitrary number of nodes appears to be a natural next step. In particular, the generalization of the greedy cooperation strategy is an interesting avenue worthy of further research. Our preliminary investigations reveal that such a strategy can get sizable performance gains, over the traditional multi-hop routing approach, in certain network configurations.

## REFERENCES

- [1] Liang-Liang Xie and P. R. Kumar, "A network information theory for wireless communication: scaling laws and optimal operation," *IEEE Trans. Inform. Theory*, vol. 50, issue 5, pp. 748 - 767, May. 2004.
- [2] S. Toumpis and A. J. Goldsmith, "Capacity regions for wireless ad hoc networks," *IEEE Trans. Wireless Comm.*, vol. 2, issue 4, pp. 736-748, Jul. 2003.
- [3] P. Gupta and P. R. Kumar, "The capacity of wireless networks," *IEEE Trans. Inform. Theory*, vol. 46, issue 2, pp. 388 - 404, Mar. 2000.
- [4] M. Grossglauser and D. N. C. Tse, "Mobility increases the capacity of ad hoc wireless networks," *IEEE/ACM Transactions on Networking*, vol. 10, issue 4, pp. 477 - 486, Aug. 2002.
- [5] T. M. Cover and A. El Gamal, "Capacity theorems for the relay channel," *IEEE Trans. Inform. Theory*, vol. 25, pp. 572-584, Sep. 1979.
- [6] T. M. Cover and J. A. Thomas, *Elements of Information Theory*. New York: Wiley, 1991.
- [7] A. El Gamal, M. Mohseni, and S. Zahedi, "On Reliable Communication over Additive White Gaussian Noise Relay Channels," Submitted to *IEEE Trans. Inform. Theory*, Dec. 2004.
- [8] E. van der Meulen, "Three-terminal communication channels", *Adv. Appl. Prob.*, vol. 3, pp. 120-154, 1971.
- [9] M. A. Khojastepour, A. Sabharwal, and B. Aazhang, "Cut-set Theorems for Multi-state Networks," Submitted to *IEEE Trans. Inform. Theory*.
- [10] G. Kramer, M. Gastpar, and P. Gupta, "Cooperative strategies and capacity theorems for relay networks," Submitted to *IEEE Trans. Inform. Theory*, Feb. 2004.
- [11] M. A. Khojastepour, A. Sabharwal, and B. Aazhang, "On the Capacity of 'Cheap' Relay Networks," in *Proc. 37th Annual Conference on Information Sciences and Systems*, Baltimore, MD, USA. Mar. 12-14, 2003.
- [12] M. A. Khojastepour, A. Sabharwal, and B. Aazhang, "On Capacity of Gaussian 'Cheap' Relay Channel," in *Proc. 2003 IEEE Global Telecommunications Conference*, San Francisco, CA, USA. Dec. 1-5, 2003, pp. 1776-1780.
- [13] A. Host-Madsen, "On the Capacity of Wireless Relaying," *Proc. 56th IEEE Vehicular Technology Conference*, Vancouver, Canada, Sept. 24-28, 2002, pp. 1333-1337.
- [14] G. Kramer, "Models and theory for relay channels with receive constraints," *Proc. 42nd Annual Allerton Conf. On Communication, Control, and Computing*, Monticello, IL, USA, Sept. 29-Oct. 1, 2004.

- [15] J. Korner and K. Marton, "General broadcast channels with degraded message sets," *IEEE Trans. Inform. Theory*, vol. 23, pp. 60-64, Jan. 1977.
- [16] R. Dabora and S. Servetto, "Broadcast channels with cooperating receivers: a downlink for the sensor reachback problem," *Proc. 2004 IEEE Intl. Symp. on Inform. Theory*, Chicago, IL, USA. June 27-July 2, 2004, pp. 176.
- [17] I. Csiszar and J. Kgrner, "Towards a General Theory of Source Networks," *IEEE Trans. Inform. Theory*, vol. 26, pp. 155-165, Mar. 1980.
- [18] J. N. Laneman, D. N. C. Tse, and G. W. Wornell, "Cooperative Diversity in Wireless Networks: Efficient Protocols and Outage Behavior," *IEEE Trans. Inform. Theory*, vol. 50, no. 12, pp. 3062-3080, Dec. 2004.
- [19] R. W. Yeung, *A First Course in Information Theory*, New York: Kluwer Academic, 2002.
- [20] M. Gastpar, G. Kramer, and P. Gupta, "The multiple-relay channel: coding and antenna-clustering capacity," *Proc. IEEE Int. Symp. Inform. Theory*, Lausanne, Switzerland, June 30- July 5, 2002, p.136.
- [21] A. Host-Madsen and J. Zhang, "Capacity bounds and power allocation for the wireless relay channel," *IEEE Trans. Inform. Theory*, vol. 51, issue 6, pp. 2020 - 2040, Jun. 2005.

## APPENDIX I

### PROOF OF LEMMA 2

To facilitate exposition we first prove the result for the discrete memoryless channel (DMC) and then progress to the Gaussian channel. In this paper, we refer to typical sequences as strong typical sequences (see [5], [6], [10] for details of strong typical sequences).

#### A. Discrete Memoryless Channel

1) *Outline:* Suppose we want to send i.i.d. source  $w(i), w(i) \in [1, M]$ , in which  $M = 2^{NR}$  to destination. Equally divide these  $2^{NR}$  messages into  $M_1 = 2^{N\alpha t R_1}$  cells, index the cell number as  $b(i)$ . Index the element in every cell as  $d(i), d(i) \in [1, M_2], M_2 = 2^{N(1-t) \cdot R_2}$ . Thus

$$2^{NR} = 2^{N\alpha t R_1} 2^{N(1-t) R_2} \quad (43)$$

that is

$$R = \alpha t R_1 + (1 - t) R_2 \quad (44)$$

The main idea is that the relay and the destination help each other to decode  $b(i)$ :

- In the first state  $m_1$ , source sends the cell index  $b(i)$  to both the relay and the destination. At this time, neither the relay nor the destination can decode this information.
- In the feedback state  $m_3$ , the destination sends compressed version of the received noisy signal to the destination. At the same time, the source sends additional information to the relay.

- At the end of the relay receive mode, the relay gets an estimation of  $b(i)$ , namely  $\hat{b}(i)$ . Thus in  $m_2$ , the relay sends its knowledge of  $\hat{b}(i)$  to the destination to help it decode  $b(i)$ . At the same time, the source sends  $d(i)$  to the destination.

2) *Random code generation:* Fix  $p(x_1|m_1), p(x_1, x_3|m_3), p(x_1, x_2|m_2), p(\hat{y}_3)$ .

- state  $m_1$ :

At the source, generate  $2^{\alpha t N R_1}$  i.i.d. length- $\alpha t N$  sequence  $\mathbf{x}_{1,m_1}$  each with probability  $p(\mathbf{x}_{1,m_1}) = \prod_{j=1}^{\alpha t N} p(x_{1j}|m_1)$ . Label these sequences as  $\mathbf{x}_{1,m_1}(b)$ , where  $b \in [1, 2^{\alpha t N R_1}]$  is called the cell index.

- state  $m_3$ :

- source node:

Generate  $2^{(1-\alpha)tNR_4}$  i.i.d. length- $(1-\alpha)tN$  codewords  $\mathbf{x}_{1,m_3}$  with  $p(\mathbf{x}_{1,m_3}) = \prod_{j=1}^{(1-\alpha)tN} p(x_{1j}|m_3)$ . Label these sequences as  $\mathbf{x}_{1,m_3}(q)$ ,  $q \in [1, 2^{(1-\alpha)tNR_4}]$ . Randomly partition the  $2^{\alpha t N R_1}$  cell indices  $\{b\}$  into  $2^{(1-\alpha)tNR_4}$  bins  $Q_q$  with  $q \in [1, 2^{(1-\alpha)tNR_4}]$ .

- destination node:

Generate  $2^{(1-\alpha)tNR_3}$  i.i.d. length- $(1-\alpha)tN$  codewords  $\mathbf{x}_{3,m_3}$  with  $p(\mathbf{x}_{3,m_3}) = \prod_{j=1}^{(1-\alpha)tN} p(x_{3j}|m_3)$ . Index them as  $\mathbf{x}_{3,m_3}(u)$ . Generate  $2^{\alpha t N \hat{R}}$  i.i.d. length- $\alpha t N$  sequences  $\hat{y}_3(z)$  with  $p(\hat{y}_3) = \prod_{j=1}^{\alpha t N} p(\hat{y}_{3j})$ . Randomly partition the set  $z \in [1, 2^{\alpha t N \hat{R}}]$  into bins  $U_u$ ,  $u \in [1, 2^{(1-\alpha)tNR_3}]$ .

- state  $m_2$ :

- relay node:

Randomly generate  $M_0 = 2^{(1-t)NR_0}$  i.i.d. length- $(1-t)N$  sequences  $\mathbf{x}_{2,m_2}$  with  $p(\mathbf{x}_{2,m_2}) = \prod_{j=1}^{(1-t)N} p(x_{2j}|m_2)$ . Index them as  $\mathbf{x}_{2,m_2}(c)$ ,  $c \in [1, 2^{(1-t)NR_0}]$ . Randomly partition the  $2^{\alpha t N R_1}$  cell indices into  $2^{(1-t)NR_0}$  bins  $C_c$ .

- source node:

Generate  $M_2 = 2^{(1-t)NR_2}$  i.i.d. length- $(1-t)N$  sequences  $\mathbf{x}_{1,m_2}$  with  $p(\mathbf{x}_{1,m_2}) = \prod_{j=1}^{(1-t)N} p(x_{1j}|x_{2j}, m_2)$  for every  $\mathbf{x}_{2,m_2}$  sequence. Index them  $\mathbf{x}_{1,m_2}(d|c)$ ,  $d \in [1, 2^{(1-t)NR_2}]$ .

3) *Encoding:* Partition the source message set into  $2^{\alpha t N R_1}$  equal-sized cells. Let  $w(i)$  be the message to be sent in block  $i$ . Suppose  $w(i)$  is the  $d(i)$ -th message in cell- $b(i)$  and the cell index  $b(i)$  is in bin- $q(i)$  and bin- $c(i)$  respectively. For brevity we drop the block index  $i$  in the following.

- state  $m_1$ :  
The source sends  $\mathbf{x}_{1,m_1}(b)$ .
- state  $m_3$ :
  - The source node knows that the cell index  $b$  is in bin- $q$ , so it sends  $\mathbf{x}_{1,m_3}(q)$ .
  - The destination first selects  $\hat{\mathbf{y}}_3(z)$  that is jointly typical with  $\mathbf{y}_{3,m_1}$ . It then sends  $\mathbf{x}_{3,m_3}(u)$  where  $z$  is in the bin  $U_u$ .
- state  $m_2$ :
  - Knowing the cell index  $b$  is in bin- $c$ , the source node sends the corresponding  $\mathbf{x}_{1,m_3}(d|c)$ .
  - Using the information received in state  $m_1$  and  $m_3$ , the relay gets an estimation of the cell index  $\hat{b}$ . Suppose  $\hat{b}$  is in bin- $\hat{c}$ . Then it sends  $\mathbf{x}_{2,m_3}(\hat{c})$ .

4) *Decoding*: In the following, code length  $N$  is chosen sufficiently large.

- at the end of  $m_1$ :  
The destination has received  $\mathbf{y}_{3,m_1}$  and it decides a sequence  $\hat{\mathbf{y}}_3(z)$  if  $(\hat{\mathbf{y}}_3(z), \mathbf{y}_{3,m_1})$  are jointly typical. There exists such a  $z$  with high probability if

$$\hat{R} \geq I(\hat{Y}_3; Y_3). \quad (45)$$

- at the end of  $m_3$ :  
At this stage, only the relay decodes the message.
  - The relay estimates  $u$  by looking for the unique  $\hat{u}$  such that  $(\mathbf{x}_{3,m_3}(\hat{u}), \mathbf{y}_{2,m_3})$  are jointly typical.  $\hat{u} = u$  with high probability if

$$R_3 \leq I(X_3; Y_2). \quad (46)$$

- Knowing  $\hat{u}$ , the relay tries to decode  $q$  by selecting the unique  $\hat{q}$  such that  $(\mathbf{x}_{1,m_3}(\hat{q}), \mathbf{x}_{3,m_3}(\hat{u}), \mathbf{y}_{2,m_3})$  are jointly typical.  $\hat{q} = q$  with high probability if

$$R_4 \leq I(X_1; Y_2 | X_3). \quad (47)$$

- The relay calculates a list  $\ell(\mathbf{y}_{2,m_1})$  such that  $z \in \ell(\mathbf{y}_{2,m_1})$  if  $(\hat{\mathbf{y}}_{3,m_1}(z), \mathbf{y}_{2,m_1})$  are jointly typical. Assuming  $u$  decoded successfully at the relay,  $\hat{z}$  is selected if it is the unique  $\hat{z} \in U_u \cap \ell(\mathbf{y}_{2,m_1})$ . Using the same argument as in [5], it can be shown that  $\hat{z} = z$  occurs with high probability if

$$\alpha t \hat{R} \leq \alpha t I(\hat{Y}_3; Y_2 | m_1) + (1 - \alpha) t R_3. \quad (48)$$

- The relay computes another list  $\ell(\mathbf{y}_{2,m_1}, \hat{\mathbf{y}}_{3,m_1})$  such that  $b \in \ell(\mathbf{y}_{2,m_1}, \hat{\mathbf{y}}_{3,m_1})$  if  $(\mathbf{x}_{1,m_1}(b), \mathbf{y}_{2,m_1}, \hat{\mathbf{y}}_{3,m_1})$  are jointly typical.
- Finally, the relay declares  $\hat{b}$  is received if it is the unique  $\hat{b} \in Q_q \cap \ell(\mathbf{y}_{2,m_1}, \hat{\mathbf{y}}_{3,m_1})$ . Using the same argument as in [5], one can show  $\hat{b} = b$  with high probability if

$$\alpha t R_1 \leq \alpha t I(X_1; \hat{Y}_3, Y_2 | m_1) + (1 - \alpha) t I(X_1; Y_2 | X_3, m_3). \quad (49)$$

- at the end of  $m_2$ :

- The destination declares that  $\hat{c}$  was sent from the relay if there exists one and only one  $\hat{c}$  such that  $(\mathbf{x}_{2,m_2}(\hat{c}), \mathbf{y}_{3,m_2})$  are jointly typical. Then  $\hat{c} = c$  with high probability if

$$R_0 \leq I(X_2; Y_3 | m_2). \quad (50)$$

- After decoding  $\hat{c}$ , the destination further declares that  $\hat{d}$  was sent from the source if it is the unique  $\hat{d}$  such that  $(\mathbf{x}_{1,m_2}(\hat{d}), \mathbf{x}_{2,m_2}(\hat{c}), \mathbf{y}_{3,m_2}, )$  are joint typical. Assuming  $c$  decoded correctly, the probability of error of  $\hat{d}$  is small if

$$R_2 \leq I(X_1; Y_3 | X_2, m_2). \quad (51)$$

- At first, the destination calculates a list  $\ell(\mathbf{y}_{3,m_1})$ , such that  $b \in \ell(\mathbf{y}_{3,m_1})$  if  $(\mathbf{x}_{1,m_1}(b), \mathbf{y}_{3,m_1})$  are jointly typical. Assuming  $c$  decoded successfully at the destination,  $\hat{b}$  is declared to be the cell index if there is a unique  $\hat{b} \in C_c \cap \ell(\mathbf{y}_{3,m_1})$ . As in [5], the decoding error is small if

$$\alpha t R_1 \leq \alpha t I(X_1; Y_3 | m_1) + (1 - t) R_0 \leq \alpha t I(X_1; Y_3 | m_1) + (1 - t) I(X_2; Y_3 | m_2). \quad (52)$$

From the cell index  $\hat{b}$  and the message index  $\hat{d}$  within the cell, the destination can recover the source message.

Combining (49) and (51), we have

$$R < \alpha t I(X_1; \hat{Y}_3, Y_2 | m_1) + (1 - \alpha) t I(X_1; Y_2 | X_3, m_3) + (1 - t) I(X_1; Y_3 | X_2, m_2). \quad (53)$$

It follows from (52) and (51) that

$$R < \alpha t I(X_1; Y_3 | m_1) + (1 - t) I(X_1, X_2; Y_3 | m_2). \quad (54)$$

From (45) and (48), we have the constraint

$$(1 - \alpha) t I(X_3; Y_2) > \alpha t I(\hat{Y}_3; Y_3 | m_1) - \alpha t I(\hat{Y}_3; Y_2 | m_1). \quad (55)$$

Thus if (53), (54), and (55) are satisfied, there exist a channel code that makes the decoding error at destination less than  $\epsilon$ .

### B. Gaussian Channel

As mentioned in [10], strong typicality does not apply to continuous random variables in general, but it does apply to the Gaussian variables. So the DMC result derived above applies to the Gaussian  $(X_1, X_2, X_3, \hat{Y})$ . Since  $\hat{Y}_3$  is a degraded version of  $Y_3$ , we write  $\hat{Y}_3 = Y_3 + Z'$  where  $Z'$  is Gaussian noise with variance  $\sigma_3^2$  (see [20], [21] for a similar analysis).

First, we examine the constraint (55) under the Gaussian inputs.

$$I(X_3; Y_2 | m_3) = h(Y_2) - h(Y_2 | X_3) = \frac{1}{2} \log \left( \frac{1}{1 - \rho_{Y_2, X_3}^2} \right). \quad (56)$$

And

$$\begin{aligned} \rho_{Y_2, X_3}^2 &= \frac{E^2\{(h_{12}X_1 + h_{23}X_3 + Z_2)X_3\}}{\text{Var}(Y_2)\text{Var}(X_3)} \\ &= \frac{\left(h_{12}r_{13}\sqrt{P_1^{(3)}} + h_{23}\sqrt{P_3^{(3)}}\right)^2}{h_{12}^2P_1^{(3)} + h_{23}^2P_3^{(3)} + \sigma^2 + 2h_{12}h_{23}r_{13}\sqrt{P_1^{(3)}P_3^{(3)}}}. \end{aligned} \quad (57)$$

So

$$I(X_3; Y_2 | m_3) = \frac{1}{2} \log \left( \frac{h_{12}^2P_1^{(3)} + h_{23}^2P_3^{(3)} + \sigma^2 + 2h_{12}h_{23}r_{13}\sqrt{P_1^{(3)}P_3^{(3)}}}{h_{12}^2(1 - r_{13}^2)P_1^{(3)} + \sigma^2} \right). \quad (58)$$

We observe that the correlation coefficient  $r_{13} = 0$  because neither the source nor the destination knows the codeword sent by the other during the feedback state. Thus, one has

$$I(X_3; Y_2 | m_3) = \frac{1}{2} \log \left( 1 + \frac{h_{23}^2P_3^{(3)}}{h_{12}^2P_1^{(3)} + \sigma^2} \right) = C \left( \frac{h_{23}^2P_3^{(3)}}{h_{12}^2P_1^{(3)} + \sigma^2} \right). \quad (59)$$

Similarly, one has

$$\begin{aligned} I(\hat{Y}_3; Y_3 | m_1) - I(\hat{Y}_3; Y_2 | m_1) &= h(\hat{Y}_3) - h(\hat{Y}_3 | Y_3) - \frac{1}{2} \log \left( \frac{1}{1 - \rho_{\hat{Y}_3, Y_2}^2} \right) \\ &= h(h_{13}X_1 + Z_3 + Z') - h(h_{13}X_1 + Z_3 + Z' | h_{13}X_1 + Z_3) \\ &\quad - \frac{1}{2} \log \left( \frac{1}{1 - \rho_{\hat{Y}_3, Y_2}^2} \right) \\ &= \frac{1}{2} \log \left( \frac{h_{13}^2P_1^{(1)} + \sigma^2 + \sigma_3^2}{\sigma_3^2} \right) - \frac{1}{2} \log \left( \frac{1}{1 - \rho_{\hat{Y}_3, Y_2}^2} \right) \end{aligned} \quad (60)$$

where

$$\begin{aligned}
\rho_{\hat{Y}_3 Y_2}^2 &= \frac{E^2(\hat{Y}_3 Y_2)}{\text{Var}(\hat{Y}_3)\text{Var}(Y_2)} \\
&= \frac{E^2\{(h_{13}X_1 + Z_3 + Z')(h_{12}X_1 + Z_2)\}}{\text{Var}(\hat{Y}_3)\text{Var}(Y_2)} \\
&= \frac{(h_{12}h_{13}P_1^{(1)})^2}{(h_{13}^2P_1^{(1)} + \sigma^2 + \sigma_3^2)(h_{12}^2P_1^{(1)} + \sigma^2)}.
\end{aligned} \tag{61}$$

so

$$I(\hat{Y}_3; Y_3|m_1) - I(\hat{Y}_3; Y_2|m_1) = \frac{1}{2} \log \left( 1 + \frac{\sigma^2}{\sigma_3^2} + \frac{1}{\sigma_3^2} \left( \frac{\sigma^2 h_{13}^2 P_1^{(1)}}{h_{12}^2 P_1^{(1)} + \sigma^2} \right) \right). \tag{62}$$

Setting

$$(1 - \alpha)tI(X_3; Y_2) = \alpha tI(\hat{Y}_3; Y_3|m_1) - \alpha tI(\hat{Y}_3; Y_2|m_1) \tag{63}$$

to solve for  $\sigma_3^2$

$$\sigma_3^2 = \frac{\sigma^2 + \frac{\sigma^2 h_{13}^2 P_1^{(1)}}{h_{12}^2 P_1^{(1)} + \sigma^2}}{\left(1 + \frac{h_{23}^2 P_1^{(3)}}{h_{12}^2 P_1^{(3)} + \sigma^2}\right)^{\frac{1-\alpha}{\alpha}} - 1}. \tag{64}$$

Next, we examine the achievable rate expression (53).

$$\begin{aligned}
I(X_1; \hat{Y}_3, Y_2|m_1) &= \frac{1}{2} \log \left( 1 + \frac{h_{12}^2 P_1^{(1)}}{\sigma^2} + \frac{h_{13}^2 P_1^{(1)}}{\sigma^2 + \sigma_3^2} \right) = C \left( \frac{h_{12}^2 P_1^{(1)}}{\sigma^2} + \frac{h_{13}^2 P_1^{(1)}}{\sigma^2 + \sigma_3^2} \right), \\
I(X_1; Y_2|X_3, m_3) &= h(Y_2|X_3, m_3) - h(Y_2|X_1, X_3, m_3) \\
&= \frac{1}{2} \log \left( 1 + \frac{h_{12}^2 P_1^{(3)}}{\sigma^2} \right) = C \left( \frac{h_{12}^2 P_1^{(3)}}{\sigma^2} \right), \\
I(X_1; Y_3|X_2, m_2) &= h(Y_3|X_2, m_2) - h(Y_3|X_1, X_2, m_2) \\
&= \frac{1}{2} \log \left( 1 + \frac{(1 - r_{12}^2) h_{13}^2 P_1^{(2)}}{\sigma^2} \right) = C \left( \frac{(1 - r_{12}^2) h_{13}^2 P_1^{(2)}}{\sigma^2} \right).
\end{aligned} \tag{65}$$

Combining them together, we get

$$\begin{aligned}
&\alpha tI(X_1; \hat{Y}_3, Y_2|m_1) + (1 - \alpha)tI(X_1; Y_2|X_3, m_3) + (1 - t)I(X_1; Y_3|X_2, m_2) \\
&= \alpha tC \left( \frac{h_{12}^2 P_1^{(1)}}{\sigma^2} + \frac{h_{13}^2 P_1^{(1)}}{\sigma^2 + \sigma_3^2} \right) + (1 - \alpha)tC \left( \frac{h_{12}^2 P_1^{(3)}}{\sigma^2} \right) + (1 - t)C \left( \frac{(1 - r_{12}^2) h_{13}^2 P_1^{(2)}}{\sigma^2} \right). \tag{66}
\end{aligned}$$

Similarly for (54), one has

$$\begin{aligned}
I(X_1; Y_3 | m_1) &= h(h_{13}X_1 + Z_3 | m_1) - h(h_{13}X_1 + Z_3 | X_1, m_1) \\
&= \frac{1}{2} \log \left( 1 + \frac{h_{13}^2 P_1^{(1)}}{\sigma^2} \right) = C \left( \frac{h_{13}^2 P_1^{(1)}}{\sigma^2} \right), \\
I(X_1, X_2; Y_3 | m_2) &= h(h_{13}^2 X_1 + h_{23} X_2 + Z_3 | m_2) - h(h_{12} X_1 + h_{23} X_2 + Z_3 | X_1, X_2, m_2) \\
&= \frac{1}{2} \log \left( 1 + \frac{h_{13}^2 P_1^{(2)} + h_{23}^2 P_2^2 + 2h_{23} r_{12} \sqrt{P_1^{(2)} P_2^{(2)}}}{\sigma^2} \right) \\
&= C \left( \frac{h_{13}^2 P_1^{(2)} + h_{23}^2 P_2^2 + 2h_{23} r_{12} \sqrt{P_1^{(2)} P_2^{(2)}}}{\sigma^2} \right),
\end{aligned} \tag{67}$$

which gives rise to

$$\begin{aligned}
&\alpha t I(X_1; Y_3 | m_1) + (1-t) I(X_1, X_2; Y_3 | m_2) \\
&= \frac{\alpha t}{2} \log \left( 1 + \frac{h_{13}^2 P_1^{(1)}}{\sigma^2} \right) + \frac{1-t}{2} \log \left( 1 + \frac{h_{13}^2 P_1^{(2)} + h_{23}^2 P_2^2 + 2h_{23} r_{12} \sqrt{P_1^{(2)} P_2^{(2)}}}{\sigma^2} \right) \\
&= \frac{\alpha t}{2} C \left( \frac{h_{13}^2 P_1^{(1)}}{\sigma^2} \right) + (1-t) C \left( \frac{h_{13}^2 P_1^{(2)} + h_{23}^2 P_2^2 + 2h_{23} r_{12} \sqrt{P_1^{(2)} P_2^{(2)}}}{\sigma^2} \right).
\end{aligned} \tag{68}$$

Setting the noise variance  $\sigma^2 = 1$ , the proof is complete.

## APPENDIX II

### PROOF OF LEMMA 3

We only show the upperbound of  $R_{FB}$ . The proof for  $R_{CF}$  is similar and thus omitted. Setting shorthand notation  $\Delta = 1 + \frac{h_{23}^2 P_3^{(3)}}{h_{12}^2 P_1^{(3)} + 1}$ , one has from (12) that

$$\begin{aligned}
1 + \frac{h_{13}^2 P_1^{(1)}}{1 + \sigma_3^2} + h_{12}^2 P_1^{(1)} &= \frac{h_{13}^2 P_1^{(1)}}{1 + \frac{(h_{12}^2 + h_{13}^2) P_1^{(1)} + 1}{(h_{12}^2 P_1^{(1)} + 1)(\Delta^{\frac{1-\alpha}{\alpha}} - 1)}} + (1 + h_{12}^2 P_1^{(1)}) \\
&= \frac{h_{13}^2 P_1^{(1)} (h_{12}^2 P_1^{(1)} + 1) (\Delta^{\frac{1-\alpha}{\alpha}} - 1)}{\Delta^{\frac{1-\alpha}{\alpha}} (h_{12}^2 P_1^{(1)} + 1) + h_{13}^2 P_1^{(1)}} + (1 + h_{12}^2 P_1^{(1)}) \\
&\leq (1 + h_{12}^2 P_1^{(1)}) \Delta^{\frac{1-\alpha}{\alpha}}.
\end{aligned} \tag{69}$$

Hence,

$$\begin{aligned}
& \alpha t C\left(\left(\frac{h_{13}^2}{1 + \sigma_3^2} + h_{12}^2\right)P_1^{(1)}\right) + (1 - \alpha)t C\left(h_{12}^2 P_1^{(3)}\right) \\
& \leq \alpha t C\left(h_{12}^2 P_1^{(1)}\right) + (1 - \alpha)t C\left(\frac{h_{23}^2 P_3^{(3)}}{h_{12}^2 P_1^{(3)} + 1}\right) + (1 - \alpha)t C\left(h_{12}^2 P_1^{(3)}\right) \\
& = \alpha t C\left(h_{12}^2 P_1^{(1)}\right) + (1 - \alpha)t C\left(h_{12}^2 P_1^{(3)} + h_{23}^2 P_3^{(3)}\right)
\end{aligned} \tag{70}$$

which proves (15).

### APPENDIX III

#### PROOF OF THEOREM 1

In view of  $R_{DF}$  in (8),  $h_{12}^2 \leq h_{13}^2$  implies that

$$R_{DF} \leq t C\left(h_{12}^2 P_1^{(1)}\right) + (1 - t) C\left((1 - r_{12}^2) h_{13}^2 P_1^{(2)}\right) \leq C\left(h_{13}^2 P\right) = R_{ro} \tag{71}$$

where we have used the total power constraint (14). To prove 2), consider the upperbound for  $R_{CF}$  in (16). Given the total power constraint  $P_1^{(2)} + P_2^{(2)} \leq P$ , it is easy to verify that  $h_{13}^2 P_1^{(2)} + h_{23}^2 P_2^{(2)} \leq \max\{h_{13}^2, h_{23}^2\} P$ . Therefore, the condition  $h_{23}^2 \leq h_{13}^2$  implies that

$$R_{CF} \leq t C\left(h_{13}^2 P_1^{(1)}\right) + (1 - t) C\left(h_{13}^2 P_1^{(2)} + h_{23}^2 P_2^{(2)}\right) \leq C\left(h_{13}^2 P\right) = R_{ro}. \tag{72}$$

The last statement of the theorem can be shown in a similar fashion using the  $R_{FB}$  upperbound in (15).

### APPENDIX IV

#### PROOF OF THEOREM 3

Since  $C(h_{12}^2 P) \geq C(h_{13}^2 P)$  by  $h_{12}^2 \geq h_{13}^2$ , the two line segments in the  $R_{DF}$  expression intersect at some optimal  $t^* \in (0, 1)$  (see Fig. 3). The corresponding rate is given by

$$R_{DF} = \frac{C\left(f_1(\theta, r_{12}, h_{13}, h_{23})P\right)C\left(h_{12}^2 P\right) - C\left(f_2(\theta, r_{12}, h_{13})P\right)C\left(h_{13}^2 P\right)}{C\left(f_1(\theta, r_{12}, h_{13}, h_{23})P\right) + C\left(h_{12}^2 P\right) - C\left(f_2(\theta, r_{12}, h_{13})P\right) - C\left(h_{13}^2 P\right)} \tag{73}$$

where we have set  $P_1^{(2)} = P \cos^2 \theta$  and  $P_2^{(2)} = P \sin^2 \theta$  according to the total power constraint. Taking  $P \rightarrow 0$ , the Taylor expansion is sufficient to establish (17). To prove the lowerbound in (17), note that  $f_1(\theta, r_{12}, h_{13}, h_{23}) \leq (h_{13}^2 + h_{23}^2)$  with equality when  $r_{12} = 1$  and  $\tan(\theta) = \frac{h_{23}}{h_{13}}$ , which, together with  $f_2(\theta, r_{12}, h_{13}) \leq h_{13}^2$ , also proves the upperbound of  $S_{DF}$  in (17).

On the other hand, as  $P \rightarrow 0$ , it is seen from (9) that  $\sigma_2^2 \rightarrow \infty$ , thus showing  $S_{CF} \leq h_{13}^2$ . The similar behavior holds for the feedback scheme, that is,  $\sigma_3^2 \rightarrow \infty$  as  $P \rightarrow 0$ , in which case  $S_{FB} \leq S_{DF}$  with the optimal  $\alpha$  approaches 1.

## APPENDIX V

### PROOF OF THEOREM 4

The results for  $G_{DF}$  and  $G_{CF}$  follows from direct computation of large  $P$  limit. We only show the last statement concerning the feedback scheme. As in the case of decode-forward, the line-crossing point gives the optimal  $t$  and the associated rate  $R_{FB}$  is given by

$$\frac{C\left(f_1(\theta, r_{12}, h_{13}, h_{23})P\right)A - C\left(f_2(\theta, r_{12}, h_{13})P\right)\alpha C\left(h_{13}^2P\right)}{C\left(f_1(\theta, r_{12}, h_{13}, h_{23})P\right) + A - C\left(f_2(\theta, r_{12}, h_{13})P\right) - \alpha C\left(h_{13}^2P\right)}, \quad (74)$$

in which

$$A = \alpha C\left(\left(\frac{h_{13}^2}{1 + \sigma_3^2} + h_{12}^2\right)P\right) + (1 - \alpha)C\left(h_{12}^2P \cos^2 \psi\right), \quad (75)$$

where we set  $P_1^{(3)} = P \cos^2 \psi$  and  $P_3^{(3)} = P \sin^2 \psi$ . Taking  $P \rightarrow \infty$ ,

$$\sigma_3^2 \rightarrow \frac{h_{12}^2 + h_{13}^2}{h_{12}^2 \left[ \left(1 + \frac{h_{23}^2}{h_{12}^2} \tan^2 \psi\right)^{\frac{1-\alpha}{\alpha}} - 1 \right]} \quad (= \sigma_3^2(\infty)). \quad (76)$$

Denote  $f_3(\psi, \alpha, h_{13}, h_{12}, h_{23}) = \alpha \log\left(\frac{h_{13}^2}{1 + \sigma_3^2(\infty)} + h_{12}^2\right) + (1 - \alpha) \log h_{12}^2 \cos^2 \psi$ , one has

$$R_{FB} \sim \frac{1}{2} \log P + \frac{\frac{1}{4}(1 - \alpha) \log f_2 \cdot \log P + \frac{1}{4} \left[ \log f_1 \cdot \log f_3 - \alpha \log f_2 \cdot \log h_{13}^2 \right]}{\frac{1-\alpha}{2} \log P + \frac{1}{2} \left[ \log f_1 + \log f_3 - \log f_2 - \alpha \log h_{13}^2 \right]}. \quad (77)$$

It follows that if  $\alpha < 1$

$$G_{FB} \leq \log f_2 \leq \log h_{13}^2 \quad (\text{relay-off}), \quad (78)$$

which forces  $\alpha = 1$ , that is,  $G_{FB} = G_{DF}$ .

## APPENDIX VI

### PROOF OF THEOREM 5

Here we only prove the part 1) of this theorem. Parts 2) - 5) follow the same lines as the corresponding results in the relay case.

To prove part 1), it suffices to show the statement for  $\alpha = 1$ . The capacity of the multicast channel without cooperation is given by  $R_{non-coop} = C(\min\{h_{13}^2, h_{12}^2\}P)$ . With the assumption that  $h_{12}^2 > h_{13}^2$ , we have  $R_{non-coop} = C(h_{13}^2P)$ .

Note that the rate expression of (27) admits the same line-crossing interpretation as in the relay case. Thus, the intersection determines the optimal rate point. Equate the two terms

$$tC(h_{12}^2P_1^{(1)}) = tC(h_{13}^2P_1^{(1)}) + (1-t)C((h_{13}^2 + h_{23}^2)P) \quad (79)$$

to solve

$$t^* = \frac{C((h_{13}^2 + h_{23}^2)P)}{C((h_{13}^2 + h_{23}^2)P) + C(h_{12}^2P) - C(h_{13}^2P)}, \quad (80)$$

which gives the corresponding rate

$$R_{DF} = \frac{C((h_{13}^2 + h_{23}^2)P)C(h_{12}^2P)}{C((h_{13}^2 + h_{23}^2)P) + C(h_{12}^2P) - C(h_{13}^2P)}. \quad (81)$$

Therefore, using  $h_{12}^2 > h_{13}^2$ , one has

$$R_{DF} - R_{non-coop} = (1-t^*)(C((h_{13}^2 + h_{23}^2)P) - C(h_{13}^2P)) > 0 \quad (82)$$

which proves the theorem.

## APPENDIX VII

### PROOF OF LEMMA 6

As Appendix I, we first prove the result for DMC case, then apply the result to the Gaussian channel.

#### A. Source coding

Randomly bin all the sequence  $S_1^K$  into  $2^{K(H(S_1|S_2)+\epsilon)}$  bins by independently generating an index  $w$  uniformly distributed on  $\{1, 2, \dots, 2^{K(H(S_1|S_2)+\epsilon)}\}$ . Let  $f_{s_1}$  be the mapping function, such that  $w = f_{s_1}(s_1^K)$ . Independently generate another bin index  $b$  for every sequence  $S_1^K$  by picking  $b$  uniformly from  $\{1, 2, \dots, 2^{KR}\}$ . Let  $B(b)$  be the set of all sequences  $S_1^K$  allocated to bin  $b$ . Thus, every source sequence is associated with two bin indexes  $\{w, b\}$ .

## B. Channel coding

### 1) Random code generation:

- At state  $m_1$ , generate  $2^{K(H(S_1|S_2)+\epsilon)}$  i.i.d. length- $N_1$  sequence  $\mathbf{x}_{1,m_1}$ , each with probability  $p(\mathbf{x}_{1,m_1}) = \prod_{j=1}^{N_1} p(x_j|m_1)$ , in which  $p(x_1|m_1)$  is the input distribution that maximizes  $I(X_1; Y_2)$ . Assign every bin index  $w$  to one sequence  $\mathbf{x}_{1,m_1}(w)$ ,  $w \in [1, 2^{K(H(S_1|S_2)+\epsilon)}]$ .
- At state  $m_2$ , randomly generate  $2^{KR}$  i.i.d. length- $N_0$   $\mathbf{x}_{2,m_2}$  at node-2, each with probability  $p(\mathbf{x}_{2,m_2}) = \prod_{j=1}^{N_0} p(x_{2j}|m_2)$ . Generate  $2^{KR}$  i.i.d. length- $N_0$   $\mathbf{x}_{1,m_2}$  at node-1, each with probability  $p(\mathbf{x}_{1,m_2}) = \prod_{j=1}^{N_0} p(x_{1j}|m_2)$ , in which  $p(x_1|m_2) = \sum_{x_2} p(x_1, x_2|m_2)$ . And  $p(x_1, x_2|m_2)$  is the input distribution that maximizes  $I(X_1, X_2; Y_3)$ . Associate every bin index  $b$  to one sequence pair  $\{\mathbf{x}_{1,m_2}(b), \mathbf{x}_{2,m_2}(b)\}$ .

2) *Coding*: Suppose we want to send source sequence  $s_1^K(i)$  at block  $i$ , and  $w(i) = f_{s_1}(s_1^K(i))$ ,  $s_1^K(i) \in B(b(i))$ . For brevity of notation, we drop block index  $i$  in the following.

- **State  $m_1$ :**  
Node-1 sends  $\mathbf{x}_{1,m_1}(w)$ .
- **State  $m_2$ :**
  - Node-1 knows  $s_1^K$  is in  $b$ , so it sends  $\mathbf{x}_{1,m_2}(b)$ .
  - At the end of state  $m_1$ , node-2 gets an estimation of  $\hat{s}_{21}^K$  (details will be given in the following), and suppose  $\hat{s}_{21}^K$  is in bin  $\hat{b}$ . Then in state  $m_2$  nodes-2 sends the corresponding  $\mathbf{x}_{2,m_2}(\hat{b})$ .

## C. Decoding

At the end of state  $m_1$ :

- **At node-2:**  
At first, node-2 looks for the one and only one  $\hat{w}$  such that  $\{\mathbf{x}_{1,m_1}(\hat{w}), \mathbf{y}_{2,m_1}\}$  are jointly typical. Then node-2 searches in the bin indexed by  $\hat{w}$  for source sequence  $\hat{s}_{21}^K$  such that  $\{\hat{s}_{21}^K, s_2^K\}$  are jointly typical. If it finds only one such sequence, it declares it has received  $\hat{s}_{21}^K$ , otherwise declares an error.
- **At node-3:**  
Node-3 calculates a list  $\ell(\mathbf{y}_{3,m_1})$ , such that  $w' \in \ell(\mathbf{y}_{3,m_1})$  if  $\{\mathbf{x}_{1,m_1}(w'), \mathbf{y}_{3,m_1}\}$  are jointly typical.

At the end of state  $m_2$ , only node-3 needs to decode:

- Step 1:

node-3 declares it receives  $\hat{b}$ , if  $\hat{b}$  is the one and only one index such that  $\{\mathbf{x}_{1,m_2}(\hat{b}), \mathbf{x}_{2,m_2}(\hat{b}), \mathbf{y}_{3,m_2}\}$  are jointly typical.

- Step 2:

node-3 searches in the bin  $B(\hat{b})$  for the one and only one source sequence  $\hat{s}_{31}^K$ , such that  $\{\hat{s}_{31}^K, s_3^K\}$  are jointly typical and  $f_{s_1}(\hat{s}_{31}^K) \in \ell(\mathbf{y}_{3,m_1})$ . If it finds such a unique one, it declares that  $\hat{s}_{31}^K$  is the source sequence. Otherwise it declares an error.

#### D. Calculation of Probability of Error

1) *Node-2*: For node-2 there are following error events:

$$E_0 = \{(s_1^K, s_2^K) \notin A_\epsilon^K\}, \quad (83)$$

$$E_1 = \{\hat{w} \neq w\}, \quad (84)$$

$$E_2 = \{\exists s_1'^K : s_1'^K \neq s_1^K, f_{s_1}(s_1'^K) = w \text{ and } (s_1'^K, s_2^K) \in A_\epsilon^K\}. \quad (85)$$

And

$$P_e^{N_1, K} = P(E_0 \cup E_1 \cup E_2) \leq P(E_0) + P(E_1|E_0^c) + P(E_2|E_0^c, E_1^c). \quad (86)$$

When  $K$  is sufficiently large, using the AEP,  $P(E_0) \rightarrow 0$ . Now consider  $P(E_1|E_0^c)$ , if channel code rate is less than the capacity, receiver will decode channel code with error probability less than  $\epsilon$ . Here, there are  $2^{K(H(S_1|S_2)+\epsilon)}$  code words, and channel code length is  $N_1$ , then the rate of channel code is  $\frac{K(H(S_1|S_2)+\epsilon)}{N_1}$ . Thus for sufficiently large  $N_1$  and  $K$ ,  $P(E_1|E_0^c) \leq \epsilon$  if

$$\frac{K(H(S_1|S_2) + \epsilon)}{N_1} < \max_{p(x_1)} I(X_1; Y_2 | m_1) = C_2, \quad (87)$$

which is the same as:

$$H(S_1|S_2) + \epsilon < \tau_1 C_2. \quad (88)$$

Because source code rate is  $H(S_1|S_2)+\epsilon$ , using the same argument as [6], one can get  $P(E_2|E_0^c, E_1^c) < \epsilon$ , if  $K$  is sufficiently large. So if (88) is satisfied, and  $N_1, K$  are sufficiently large, there exists a source-channel code that make the error probability at node-2

$$P_e^{N_1, K} = P(\hat{s}_{21}^K \neq s_1^K) \leq 3\epsilon. \quad (89)$$

2) *Node-3*: For node-3, there are following error events:

$$E_0 = \{(s_1^K, s_3^K) \notin A_\epsilon^K\}, \quad (90)$$

$$E_1 = \{\text{node 2 can not decode successfully}\}, \quad (91)$$

$$E_2 = \{\hat{b} \neq b\}, \quad (92)$$

$$E_3 = \{\exists s_1'^K : s_1'^K \neq s_1^K, f_{s_1}(s_1'^K) \in \ell(\mathbf{y}_3|m_1), s_1'^K \in B(\hat{b}), (s_1'^K, s_3^K) \in A_\epsilon^K\}. \quad (93)$$

$$P_e^{N,K} = P(E_0 \cup E_1 \cup E_2 \cup E_3) \leq P(E_0) + P(E_1) + P(E_2|E_0^c, E_1^c) + P(E_3|E_0^c, E_1^c, E_2^c). \quad (94)$$

When  $K$  is sufficiently large,  $P(E_0) \rightarrow 0$ . And if (88) is satisfied,  $P(E_1) \leq 3\epsilon$ . Now consider  $P(E_2|E_0^c, E_1^c)$ , the channel code rate is  $\frac{KR}{N_0}$ . So,  $P(E_2|E_0^c, E_1^c) \leq \epsilon$  for sufficiently large  $N_0$ , if

$$\frac{KR}{N_0} \leq \max_{p(x_1, x_2)} I(X_1, X_2; Y_3) = C_{(1,2)-3}, \quad (95)$$

that is,

$$R \leq \tau_0 C_{(1,2)-3}. \quad (96)$$

Now consider  $P(E_3|E_0^c, E_1^c, E_2^c)$ :

$$\begin{aligned} P(E_3|E_0^c, E_1^c, E_2^c) &= P(\exists s_1'^K : s_1'^K \neq s_1^K, f_{s_1}(s_1'^K) \in \ell(\mathbf{Y}_3|m_1), s_1'^K \in B(b), (s_1'^K, s_3^K) \in A_\epsilon^K) \\ &= \sum_{(s_1^K, s_3^K)} p(s_1^K, s_3^K) P(\exists s_1'^K \neq s_1^K, f_{s_1}(s_1'^K) \in \ell(\mathbf{y}_3|m_1), s_1'^K \in B(b), (s_1'^K, s_3^K) \in A_\epsilon^K) \\ &\leq \sum_{(s_1^K, s_3^K)} p(s_1^K, s_3^K) \sum_{s_1'^K \neq s_1^K \text{ and } (s_1'^K, s_3^K) \in A_\epsilon^K} P(f_{s_1}(s_1'^K) \in \ell(\mathbf{y}_3|m_1), s_1'^K \in B(b)) \\ &= \sum_{(s_1^K, s_3^K)} p(s_1^K, s_3^K) \sum_{s_1'^K \neq s_1^K \text{ and } (s_1'^K, s_3^K) \in A_\epsilon^K} P(f_{s_1}(s_1'^K) \in \ell(\mathbf{y}_3|m_1)) P(s_1'^K \in B(b)) \\ &\leq \sum_{(s_1^K, s_3^K)} p(s_1^K, s_3^K) 2^{-K(H(S_1|S_2)+\epsilon)} \|\ell(\mathbf{y}_3|m_1)\| 2^{-KR} \|A_\epsilon(S_1^K|s_3^K)\| \\ &\leq 2^{-K(H(S_1|S_2)+\epsilon)} E\{\|\ell(\mathbf{y}_3|m_1)\|\} 2^{-KR} 2^{K(H(S_1|S_3)+\epsilon)}. \end{aligned} \quad (97)$$

Follow the same steps in the [5], one has  $E\{\|\ell(\mathbf{y}_3|m_1)\|\} \leq 1 + 2^{K(H(S_1|S_2)+\epsilon)}2^{-N_1(I(X_1;Y_3|m_1)-7\epsilon)}$ .

So

$$\begin{aligned} P(E_3|E_0^c, E_1^c, E_2^c) &\leq 2^{-K(H(S_1|S_2)+\epsilon)}(1 + 2^{K(H(S_1|S_2)+\epsilon)}2^{-N_1(I(X_1;Y_3|m_1)-7\epsilon)})2^{-KR}2^{K(H(S_1|S_3)+\epsilon)} \\ &= 2^{-K\{R-(H(S_1|S_3)+\epsilon)+(H(S_1|S_2)+\epsilon)\}} + 2^{-K\{R+\frac{N_1}{K}(I(X_1;Y_3|m_1)-7\epsilon)-(H(S_1|S_3)+\epsilon)\}} \end{aligned} \quad (98)$$

So if

$$R > H(S_1|S_3) + \epsilon - (H(S_1|S_2) + \epsilon), \quad (99)$$

and

$$R > H(S_1|S_3) + \epsilon - \frac{N_1}{K}(I(X_1;Y_3|m_1) - 7\epsilon) > H(S_1|S_3) + \epsilon - \tau_1 I(X_1;Y_3|m_1), \quad (100)$$

and  $K$  is sufficiently large,  $P(E_3|E_0^c, E_1^c, E_2^c) \leq \epsilon$ . Together with (88) and (96), one can get

$$H(S_1|S_3) + \epsilon - \frac{\min\{I(X_1;Y_3|m_1) - 7\epsilon, C_2\}(H(S_1|S_2) + \epsilon)}{C_2} \leq \tau_0 C_{(1,2)-3}. \quad (101)$$

Thus, if both (101) and (88) are satisfied, there exists a source-channel code that makes the error probability at node-3  $P_e^{N,K} < 6\epsilon$ .

Next step is to apply the result to the Gaussian channel. In this case, we have

$$\begin{aligned} C_2 &= C(h_{12}^2 P), \\ I(X_1;Y_3|m_1) &= C(h_{13}^2 P), \\ C_{(1,2)-3} &= C((h_{13}^2 + h_{23}^2)P). \end{aligned} \quad (102)$$

Inserting (102) to (101) and (88) completes the proof.

## APPENDIX VIII

### PROOF OF THEOREM 7

Part 1) and 2) of this theorem follow straightforward limit calculation, we only prove part 3).

The assumption  $\tau_{ex,2} < \tau_{ex,3}$  becomes  $\frac{H(S_1|S_2)}{h_{12}^2} < \frac{H(S_1|S_3)}{h_{13}^2}$  when  $P \rightarrow 0$ . Under this assumption, there are two different cases corresponding to different cost function for the benchmark scheme:  $H(S_1|S_2) > H(S_1|S_3)$  and  $H(S_1|S_2) < H(S_1|S_2)$ .

When  $H(S_1|S_2) > H(S_1|S_3)$ , in which case  $h_{12}^2 > h_{13}^2$  and

$$E_{1,m} = \frac{2}{\log e} \left( \frac{H(S_1|S_2)}{h_{12}^2} + \left( \frac{1}{h_{13}^2} - \frac{1}{h_{12}^2} \right)^+ H(S_1|S_3) \right). \quad (103)$$

$$\begin{aligned}
E_{2,m} &= \frac{2}{\log e} \left( \frac{H(S_1|S_2)}{h_{12}^2} + \frac{h_{12}^2 H(S_1|S_3) - h_{13}^2 H(S_1|S_2)}{(h_{13}^2 + h_{23}^2)h_{12}^2} \right) \\
&< \frac{2}{\log e} \left( \frac{H(S_1|S_2)}{h_{12}^2} + \frac{h_{12}^2 H(S_1|S_3) - h_{13}^2 H(S_1|S_3)}{(h_{13}^2 + h_{23}^2)h_{12}^2} \right) \\
&< \frac{2}{\log e} \left( \frac{H(S_1|S_2)}{h_{12}^2} + \frac{h_{12}^2 H(S_1|S_3) - h_{13}^2 H(S_1|S_3)}{h_{13}^2 h_{12}^2} \right) \\
&\leq \frac{2}{\log e} \left( \frac{H(S_1|S_2)}{h_{12}^2} + \left( \frac{1}{h_{13}^2} - \frac{1}{h_{12}^2} \right)^+ H(S_1|S_3) \right) \\
&= E_{1,m}.
\end{aligned} \tag{104}$$

When  $H(S_1|S_2) > H(S_1|S_3)$ ,

$$E_{1,m} = \frac{2}{\log e} \left( \frac{H(S_1|S_3)}{h_{13}^2} + \left( \frac{1}{h_{12}^2} - \frac{1}{h_{13}^2} \right)^+ H(S_1|S_2) \right), \tag{105}$$

so

$$\begin{aligned}
E_{2,m} &= \frac{2}{\log e} \left( \frac{H(S_1|S_2)}{h_{12}^2} + \frac{h_{12}^2 H(S_1|S_3) - \min\{h_{13}^2, h_{12}^2\} H(S_1|S_2)}{(h_{13}^2 + h_{23}^2)h_{12}^2} \right) \\
&< \frac{2}{\log e} \left( \frac{H(S_1|S_2)}{h_{12}^2} + \frac{h_{12}^2 H(S_1|S_3) - \min\{h_{13}^2, h_{12}^2\} H(S_1|S_2)}{h_{13}^2 h_{12}^2} \right) \\
&= \frac{2}{\log e} \left( \frac{H(S_1|S_2)}{h_{12}^2} + \frac{H(S_1|S_3)}{h_{13}^2} - \min\left\{ \frac{1}{h_{13}^2}, \frac{1}{h_{12}^2} \right\} H(S_1|S_2) \right) \\
&= \frac{2}{\log e} \left( \frac{H(S_1|S_3)}{h_{13}^2} + \left( \frac{1}{h_{12}^2} - \frac{1}{h_{13}^2} \right)^+ H(S_1|S_2) \right) \\
&= E_{1,m}.
\end{aligned} \tag{106}$$

## APPENDIX IX

### PROOF OF THEOREM 8

For part 1) of this theorem, without loss of generality, we only prove the case when  $h_{23}^2 \rightarrow \infty$ . In this case,  $\lim_{h_{23}^2 \rightarrow \infty} \tau_{2,gen} = \lim_{h_{23}^2 \rightarrow \infty} \tau_{3,gen} = 0$ ,  $\tau_{gen} = \tau_{1,gen}$ . In the following, we will show that the genie-aided bound could be achieved using the following multicast order  $2 \rightarrow 3 \rightarrow 1$ .

When node-2 multicasts  $S_2^K$  to both node-3 and node-1 using the proposed cooperative multicast with side-information scheme, from Lemma 7 we know it requires

$$\tau_{2-(3,1)} = \frac{H(S_2|S_3)}{R_{CFr1d3}(\alpha)} + \frac{H(S_2|S_1) - \alpha H(S_2|S_3) \frac{\min\{I(X_2;Y_1), I(X_2; \hat{Y}_1, Y_3)\}}{R_{CFr1d3}(\alpha)}}{C((h_{12}^2 + h_{13}^2)P)}.$$

$R_{CFr1d3}$  means the achievable rate of the following relay channel using Compress-Forward scheme: node-2 is the source, node-1 acts as relay that spends  $1 - \alpha$  part of the time in helping destination using CF scheme, and node-3 acts as the destination.

Next consider node-3 multicasts  $S_3^K$  to both node-1, node-2. At this time, node-1 already has  $S_1, S_2$ , thus this step requires

$$\tau_{3-(2,1)} = \frac{H(S_3|S_2)}{R_{CFr1d2}(\alpha)} + \frac{H(S_3|S_1, S_2) - \alpha H(S_2|S_3) \frac{\min\{I(X_3; Y_1), I(X_3; \hat{Y}_1, Y_2)\}}{R_{CFr1d2}(\alpha)}}{C((h_{12}^2 + h_{13}^2)P)}.$$

Final step, node-1 multicasts  $H(S_1|S_2, S_3)$  to both node-2, node-3 using the greedy multicast scheme developed in the multicast section, this step requires  $\tau_{1-(2,3)} = \frac{H(S_1|S_2, S_3)}{R_g}$ .

Thus, the total bandwidth expansion factor of this scheme is

$$\tau = \tau_{2-(3,1)} + \tau_{3-(1,2)} + \tau_{1-(2,3)}. \quad (107)$$

Based on the results on the relay channel and multicast channel  $h_{23}^2 \rightarrow \infty, R_{CFr1d3} \rightarrow \infty, R_{CFr1d2} \rightarrow \infty, \lim_{h_{23}^2 \rightarrow \infty} R_g = C((h_{12}^2 + h_{13}^2)P)$ . Then

$$\begin{aligned} \lim_{h_{23}^2 \rightarrow \infty} \tau &= \frac{H(S_2|S_1) + H(S_3|S_1, S_2) + H(S_1|S_2, S_3)}{C((h_{12}^2 + h_{13}^2)P)} \\ &= \frac{H(S_2, S_3|S_1) + H(S_1|S_2, S_3)}{C((h_{12}^2 + h_{13}^2)P)} = \tau_{1,gen} = \tau_{gen}. \end{aligned} \quad (108)$$

To prove the second part of this theorem, without loss of generality, suppose  $1 \rightarrow 2 \rightarrow 3$  is the optimal multicast order for the scheme that uses broadcast with degraded information set. Then, just use the same order for the cooperative source-channel coding scheme based multicast with side-information. Theorem 7 shows that at every multicast step, the cooperative source-channel coding scheme outperforms the broadcast with degraded information set. Thus even with this not necessarily optimal order, the cooperative source-channel coding scheme outperforms the scheme that uses broadcast with degraded information set with optimal order.

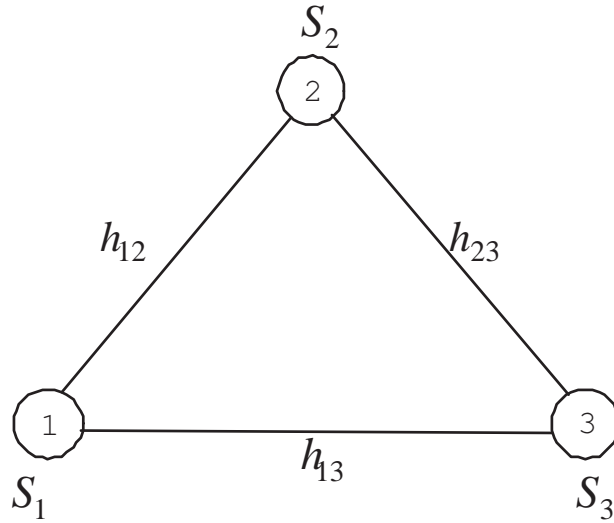


Fig. 1. An illustration of the three-node (half-duplex) wireless network. Each node may be interested in a subset or all the observation variables distributed across the network.

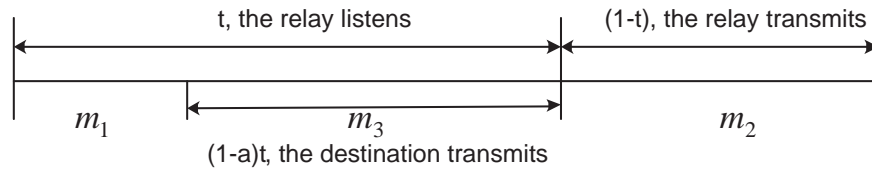


Fig. 2. The operation sequence of the half-duplex relay channel with realistic feedback.

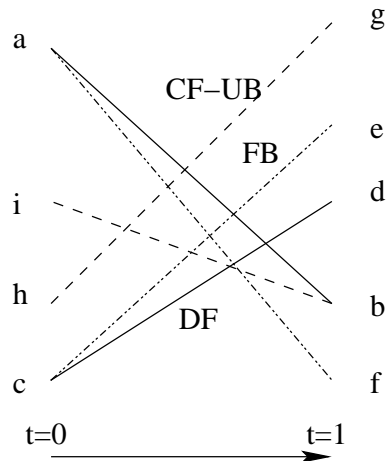


Fig. 3. A geometric representation of FB-, DF- and CF-relay schemes. The solid lines are for  $R_{DF}$  in (8), the dash-dotted for  $R_{FB}$  in (12), and the dashed for the upperbound of  $R_{CF}$  in (16). The various endpoints in the figure are (a)  $C(h_{13}^2 P_1^{(2)} + 2r_{12} h_{13} h_{23} \sqrt{P_1^{(2)} P_2^{(2)} + h_{23}^2 P_2^{(2)}})$ , (b)  $C(h_{13}^2 P_1^{(1)})$ , (c)  $C((1 - r_{12}^2) h_{13}^2 P_1^{(2)})$ , (d)  $C(h_{12}^2 P_1^{(1)})$ , (e)  $\alpha C((\frac{h_{13}^2}{1 + \sigma_3^2} + h_{12}^2) P_1^{(1)}) + (1 - \alpha) C(h_{12}^2 P_1^{(3)})$ , (f)  $\alpha C(h_{13}^2 P_1^{(1)})$ , (g)  $C((h_{13}^2 + h_{12}^2) P_1^{(1)})$ , (h)  $C(h_{13}^2 P_1^{(2)})$ , and (i)  $C(h_{13}^2 P_1^{(2)} + h_{23}^2 P_2^{(2)})$ .



Fig. 4. Orthogonal transmission: the source spends  $t$  part of the time to transmit, the relay uses the remaining  $1 - t$  part of the time to transmit.

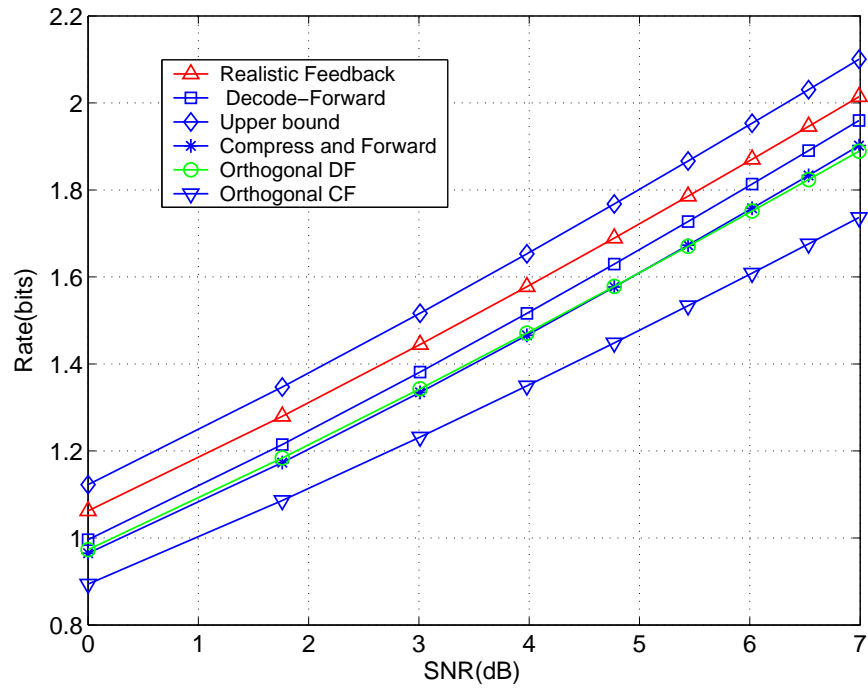


Fig. 5. The achievable rate of various schemes in the half-duplex relay channel,  $h_{12} = 1.8, h_{13} = 1, h_{23} = 23dB$ .

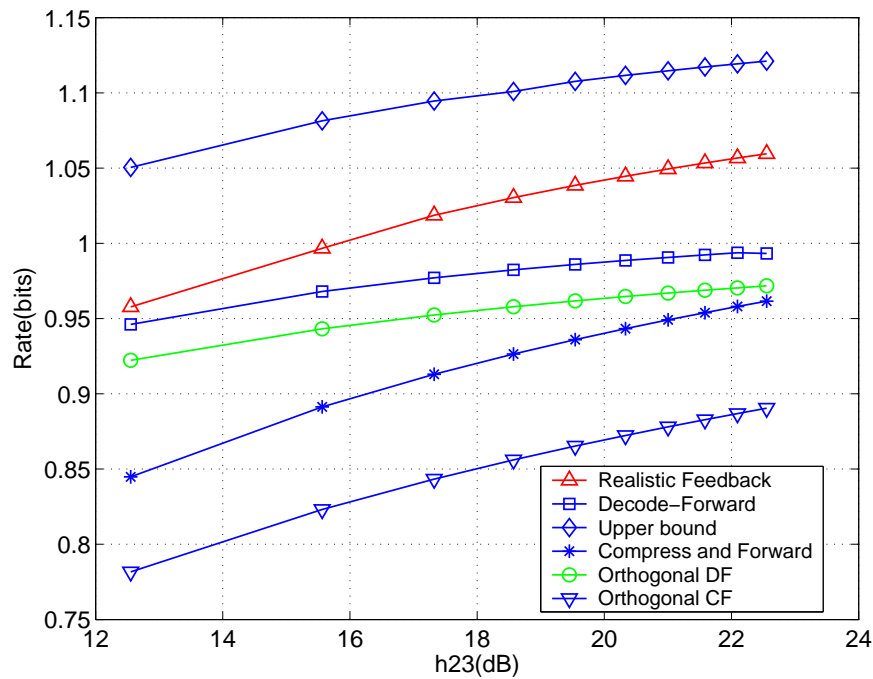


Fig. 6. The achievable rate of various schemes in the half-duplex relay channel,  $h_{12} = 1.8, h_{13} = 1, SNR = 0dB$ .

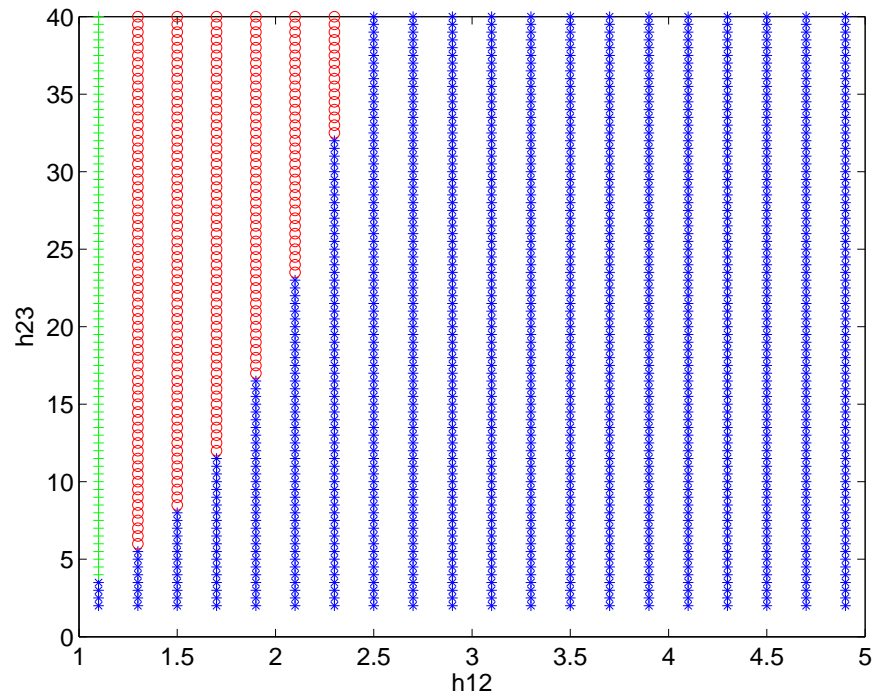


Fig. 7. Optimal regions for decode-and-forward (denoted by '\*'), compress-and-forward (denoted by '+'), and feedback strategy (denoted by 'o'), when  $\text{SNR} = 3\text{dB}$ .

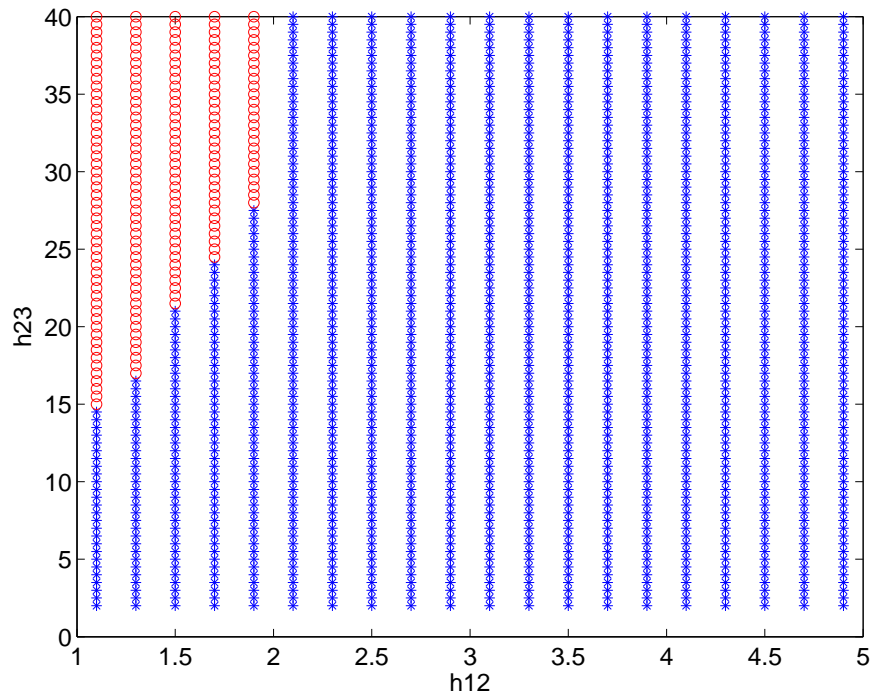


Fig. 8. Optimal regions for decode-and-forward (denoted by '\*'), compress-and-forward (denoted by '+'), and feedback (denoted by 'o'), when  $\text{SNR} = -20\text{dB}$ .

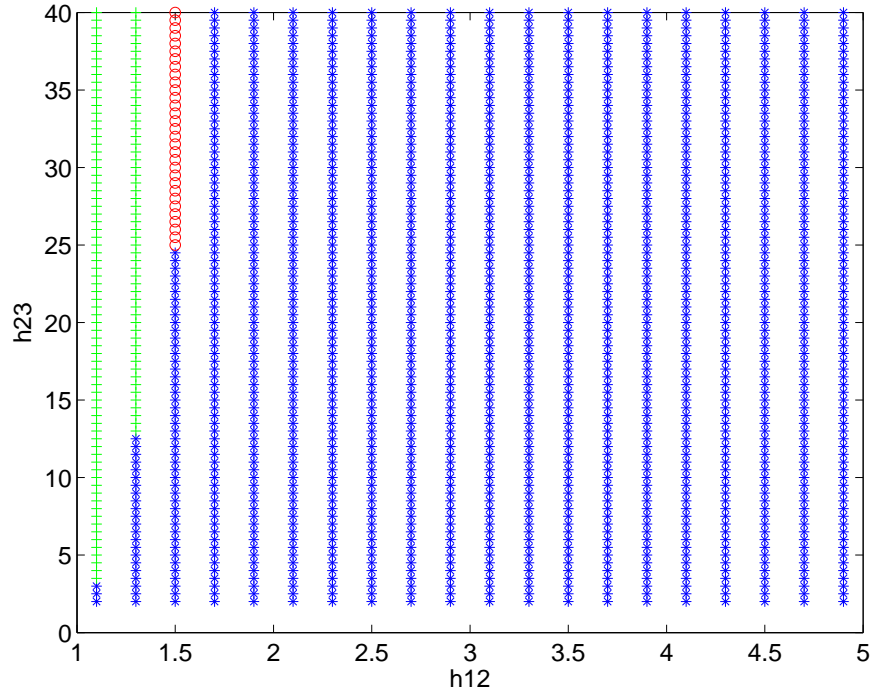


Fig. 9. Optimal regions for decode-and-forward (denoted by '\*'), compress-and-forward (denoted by '+'), and feedback strategy (denoted by 'o'), when  $\text{SNR} = 20\text{dB}$ .

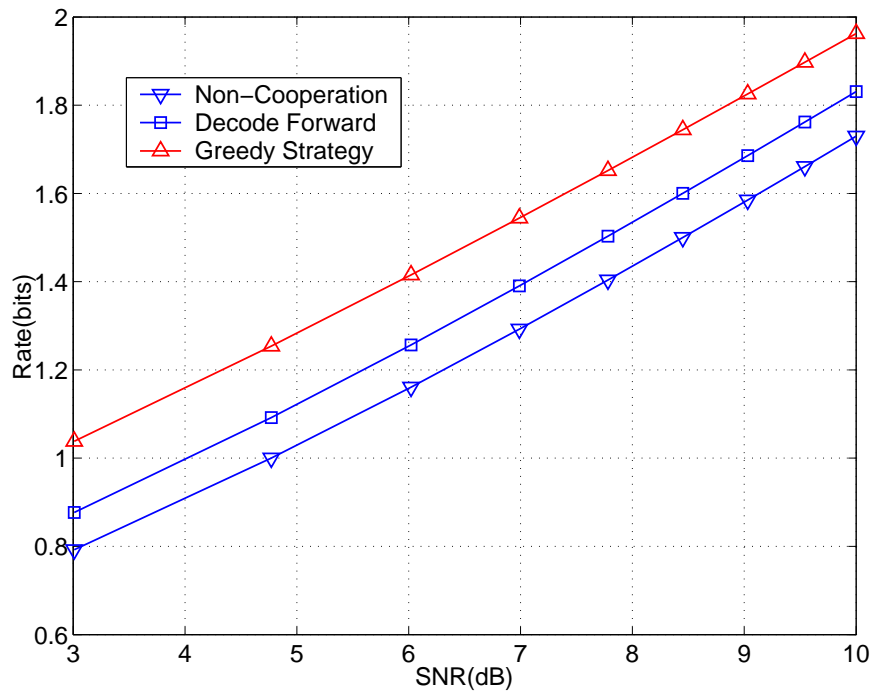


Fig. 10. The achievable rate of various schemes in the multicast channel,  $h_{12} = 1.1$ ,  $h_{13} = 1$ , and  $h_{23} = 23\text{dB}$ .

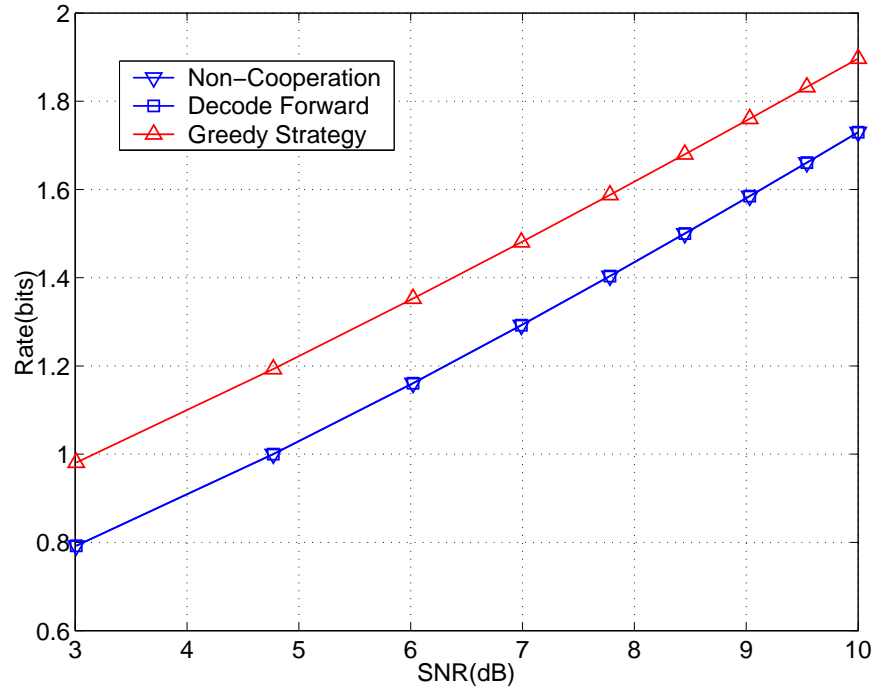


Fig. 11. The achievable rate of various schemes in the multicast channel,  $h_{12} = 1$ ,  $h_{13} = 1$ , and  $h_{23} = 23dB$ .

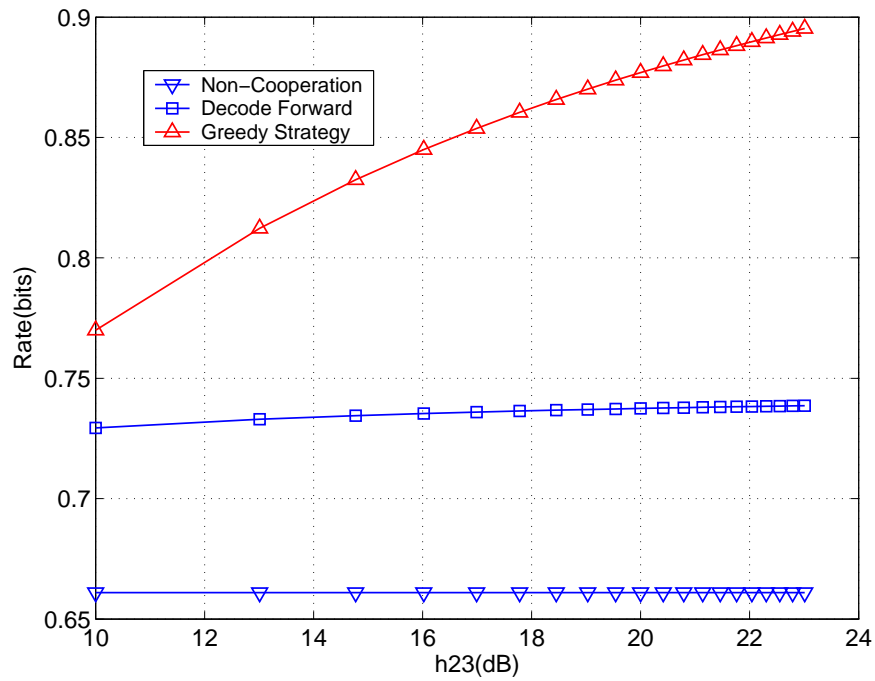


Fig. 12. The achievable rate of various schemes in the multicast channel,  $h_{12} = 1.1$ ,  $h_{13} = 1$ , and  $SNR = 1.8dB$ .

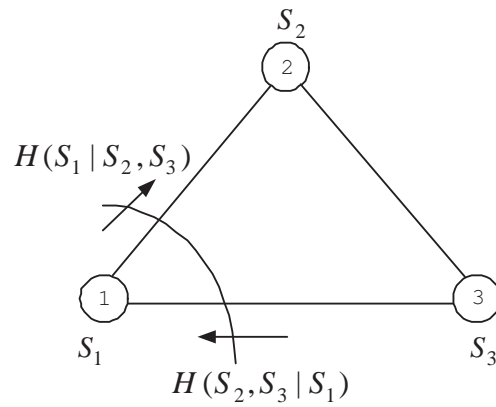


Fig. 13. The genie-aided bound in node-1, in which node-2 and node-3 can fully cooperate with each other.

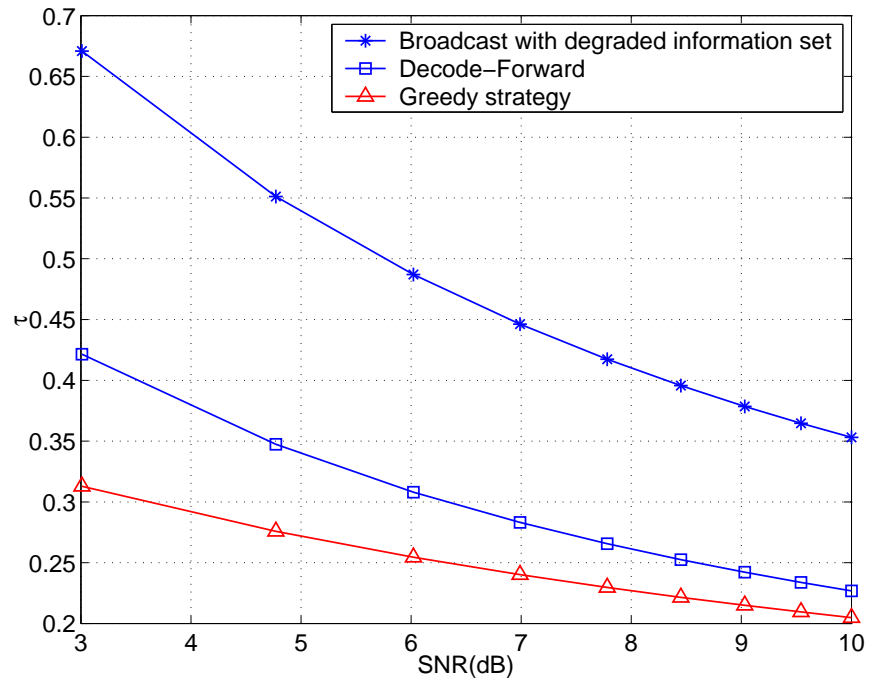


Fig. 14. The bandwidth expansion factor of various schemes in the multicast channel with side-information,  $h_{12} = 2, h_{13} = 1, h_{23} = 90, H(S_1|S_2) = 0.9, H(S_1|S_3) = 0.3$ .

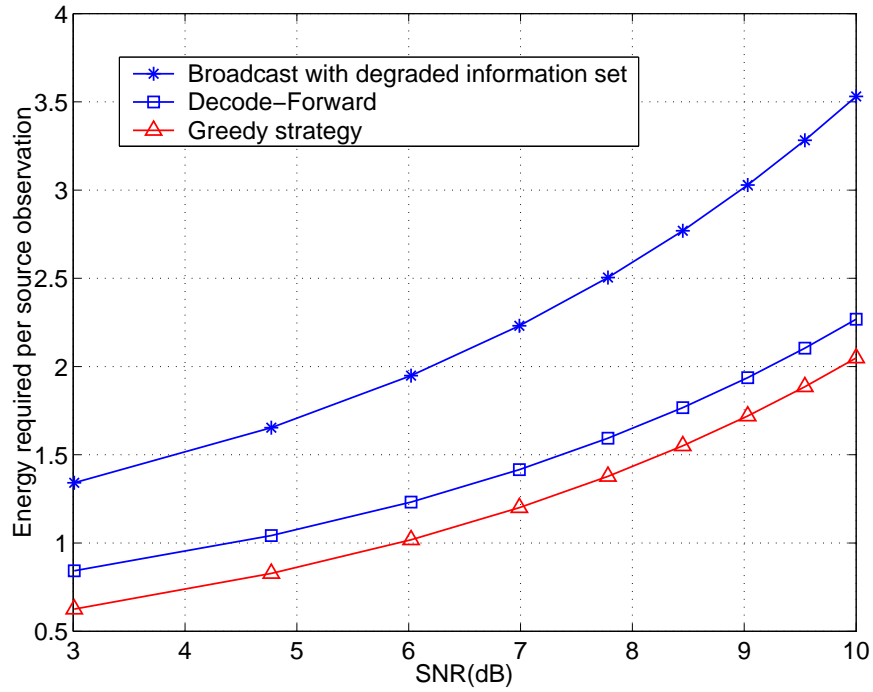


Fig. 15. The energy required per source observation of various schemes in the multicast channel with side-information,  $h_{12} = 2, h_{13} = 1, h_{23} = 90, H(S_1|S_2) = 0.9, H(S_1|S_3) = 0.3$ .

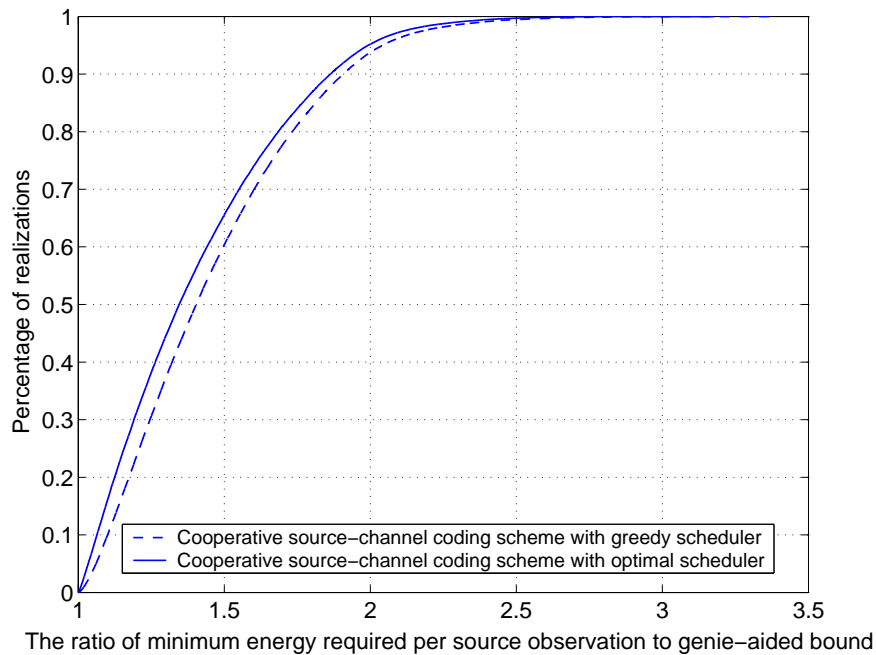


Fig. 16. The ratio of the energy required per source observation of the cooperative source-channel coding scheme to the genie aid bound.

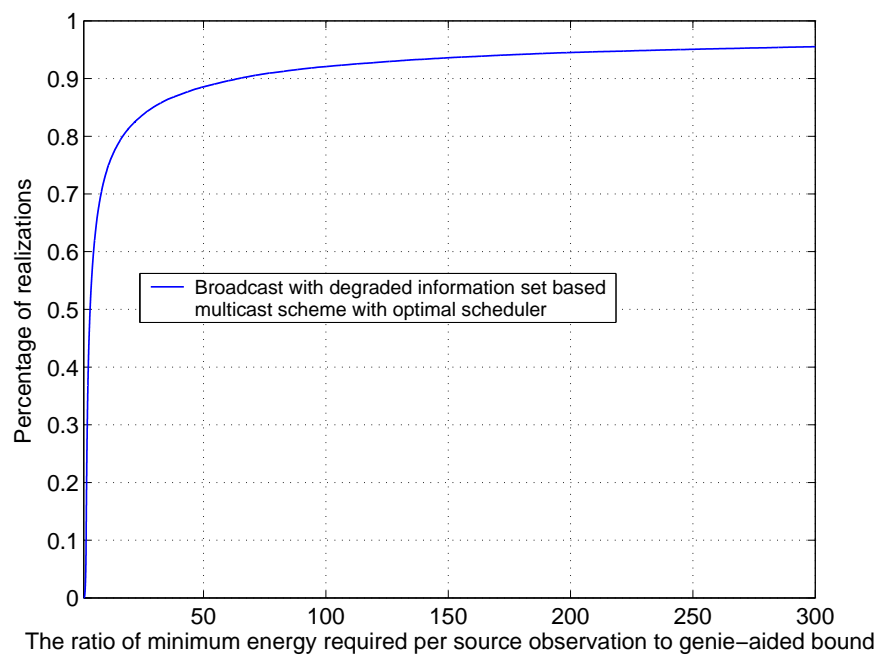


Fig. 17. The ratio of the energy required per source observation of the broadcast with degraded information set based multicast with optimal scheduler to the genie aid bound.